Technische Universität München
TUM School of Medicine and Health

Exploitation of the stress response of the hematopoietic niche to control cell cycle progression of hematopoietic stem cells

Renate Ilona Bachmann

Vollständiger Abdruck der von der TUM School of Medicine and Health der Technischen Universität München zur Erlangung einer

Doktorin der Medizinischen Wissenschaft (Dr.med.sci.)

genehmigten Dissertation.

Vorsitz: Prof. Dr. Michael Joner

Prüfende der Dissertation:

1. apl. Prof. Dr. Robert Oostendorp
2. Prof. Dr. Hendrik Sager

Die Dissertation wurde am 02.01.2025 bei der Technischen Universität München eingereicht und durch die TUM School of Medicine and Health am 18.06.2025 angenommen.

Table of Contents

List of Abbreviations

AGM	Aorta-gonad-mesonephros
ALL	acute lymphatic leukemia
BM	Bone marrow
CAR	CXCL12-abundant reticular cells
cDNA	complementary DNA
CLL	chronic lymphocytic leukemia
CML	chronic myeloid leukemia
CMP	common myeloid progenitors
CXCL12	C-X-C motif chemokine ligand 12
CTSK	Cathepsin K
DNA	Deoxyribonucleic acid
dsDNA	double-stranded DNA
DKK1	Dickkopf-related protein 1
dNTP	deoxy nucleoside triphosphate
DOCK2	Dedicator of cytogenesis 2
FZD	Frizzled
GSK3	Glykogen synthase kinase 3
GEF	Guanidine exchange factor
HSC	Hematopoietic stem cell
IC50	half-maximal inhibitory concentration
IL	Interleukin
IT-HSC	Intermediate-term hematopoietic stem cell
LRP	Low-density lipoprotein-related protein
LMMP	Lymphoid multipotent progenitors
LT-HSC	Long-term hematopoietic stem cell
LSK	$Lineage^{-}SCA\text{-}1^{+}kit^{+}$
MPP	Multipotent progenitors
MSPC	Mesenchymal stem and progenitor cell
PB	Peripheral blood
PCP	Planar cell polarity
PIP5K1a	Phosphatidylinositol-4-phosphate 5-kinase type 1 alpha
PLCE1	Phospholipase C epsilon 1
RNA	Ribonucleic acid
RT-qPCR	real-time quantitative polymerase chain reaction
SCF	Stem cell factor
SFRP1	Secreted frizzled-related protein 1
SLAM	Signal lymphocyte activating molecule
SPL	Spleen
ST-HSC	Short-term hematopoietic stem cell
THY	Thymus
TPO	Thrombopoietin
WNT	Wingless Integrase-1

1. Introduction

1.1 Hematopoiesis and stem cell hierarchy

A highly regenerative organ, blood produces approximately 10^{12} cells each day (Pinho & Frenette, 2019). These cells include various specialized lineages such as granulocytes, monocytes, dendritic cells, T- and B-lymphocytes, natural killer cells, erythrocytes, and platelets. They are essential for vital functions like oxygen transport, innate and adaptive immunity, and wound healing. Most of them are short-lived cell types and originate from the rare population of (long-term) hematopoietic stem cells (LT-HSCs) in the bone marrow (BM). The LT-HSCs in turn have two fundamental characteristics: the competence to unlimited self-renewal and to replenish all blood cell types throughout life (Osawa et al., 1996).

In mice, the LT-HSCs are characterized by the ability to engraft and repopulate in at least two rounds of transplantation assays (Laurenti & Gottgens, 2018). The lineage and maturity of HSC can be defined by their distinct cell surface markers. Early murine HSC are identified by expression of the stem cell antigen-1 (Sca-1, Ly6A/E) and the c-Kit- receptor (c-Kit, CD117) in absence of the cell surface markers normally expressed on mature, lineage-committed hematopoietic stem cells such as CD4, CD8, B220, Ter119, CD11b, Gr-1 (Osawa et al., 1996), therefore called $Lin^{-}Sca^{+}Kit^{+}$ (LSK) cells. LT-HSCs additionally lack expression of the surface antigen CD34, FLT3 and the differentiation marker CD48, but express the CD150 surface lymphocyte activation marker (SLAM) phenotype (Kiel et al., 2005) and the protein C receptor EPCR/PROCR (Balazs et al., 2006). About 15% of the LT-HSCs are dormant, they reside in the G0 phase of the cell cycle, and do not support steady-state hematopoiesis (Kiel et al., 2007; Wilson et al., 2007).

There are multiple other subpopulations of HSCs, including intermediate-term HSCs and short-term HSCs (ST-HSCs), that differ by the duration and robustness of their multilineage reconstitution abilities and express both CD34 and FLT3 (Benveniste et al., 2010). Multipotent progenitors (MPPs) are characterized by the acquisition of CD48 (Wilson et al., 2007) and the loss of CD150 (Oguro et al.,

2013). They are the last in the stem cell hierarchy to give multilineage repopulation and exhaust within few weeks in transplantation experiments (Kent et al., 2016).

The MPP generate precursors that commit to unilineage differentiation, the lymphoid multipotent progenitors (LMPP) that produce lymphoid cells and the common myeloid progenitors (CMP). The latter differentiate into granulocyte-monocyte precursors and megakaryocyte-erythrocyte-precursors. Hence, MPP sustain steady-state hematopoiesis.

Figure 1 provides an overview of the hierarchical system of the classical hematopoiesis in mice according to identified cell surface markers. However, new evidence of non-hierarchically coexisting HSCs with alternative differentiation pathways challenges the established hierarchical model (Carrelha et al., 2024; Zhang et al., 2018).

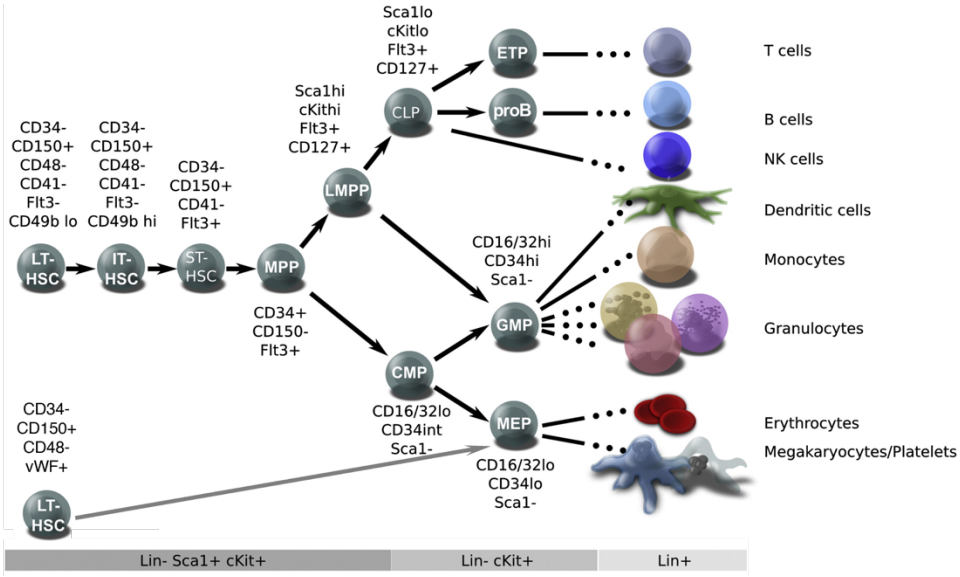

Figure 1 Cell surface markers during hematopoiesis. Modified from Doulatov et al. (Doulatov et al., 2012)

1.2 The bone marrow niche: The microenvironment of adult hematopoietic stem cells

Our understanding of the stem cell hierarchy and the identification of HSC subsets by distinct cell surface markers is in contrast with their substantial functional heterogeneity despite minimal immunophenotypic differences (Rodriguez-Fraticelli & Camargo, 2021).

Single cell transplantation experiments show that HSCs repopulate different lineages in varying proportions. Each HSC has unique lineage production patterns (Dykstra et al., 2007). These so-called lineage biases have been confirmed through in situ barcoding methods (Rodriguez-Fraticelli et al., 2018). The biases occur not only under hematopoietic stress during transplantation but also in (natural) steady-state hematopoiesis. Biased HSC respond differently to cytokines like TGF-β and IL-7, which might explain their specific lineage outputs (Challen et al., 2010), suggesting that this heterogeneity is significantly influenced by the HSC microenvironment, the hematopoietic niche.

The niche consists of many different cell types that are critical regulators of HSCs through extrinsic signals like adhesion molecules, cytokines or growth factors (Schreck et al., 2014). The main function of the hematopoietic niche is to ensure the survival and self-renewal of the HSC pool, therefore keeping HSCs in a dormant state. In the adult mammal, hematopoiesis primarily occurs in the bone marrow (BM), where HSCs are mainly found within the perivascular niche, with only a few of them residing near the endosteum. The perivascular niche consists of a vascular network of arterioles and sinusoids—low-pressure capillaries with a fenestrated endothelium. Residing here, HSCs are surrounded by various cell types that regulate them via direct cell-cell-contact or through secretion of cytokines (Deng et al., 2024; Wei & Frenette, 2018). The proximity to the blood vessel endothelium facilitates rapid entry of the HSCs into circulation during hematological stress.

The perivascular niche includes leptin receptor-positive (LEP-R+) stromal cells, CXCL12-abundant reticular (CAR) mesenchymal stem cells (MSC), and Nestin+

multipotent stromal cells (Greenbaum et al., 2013; Mendez-Ferrer et al., 2010). These cell types secrete CXCL12 and stem cell factor, both critical niche factors essential for HSC homing and maintenance, making them primary regulators of hematopoiesis (Ding et al., 2012; Omatsu et al., 2010; Sugiyama et al., 2006). Osteolineage cells, such as osteoblasts and osteoclasts are involved in the regulation of HSCs but primarily maintain common lymphoid progenitors. Adipocytes are believed to inhibit the niche, while adrenergic nerves can also guide HSC mobilization. Additionally, the progeny of HSCs, particularly megakaryocytes and regulatory T-cells, can modulate HSCs dormancy via negative feedback mechanisms.

The endosteal region of the trabecular bone area harbors only few HSCs. These are thought to be the quiescent LT-HSCs, that attach to N-cadherin-positive osteoblasts (Wilson et al., 2007; Xie et al., 2009).

Besides the critical niche factors CXCL12 and SCF, there are multiple other secreted molecules that impact HSC behavior relevantly. Components of WNT (Wingless integrase-1) signaling, like Secreted frizzled-related protein 1 (SFRP1) and Dickkopf-related protein 1 (DKK1) regulate HSC fate (Frobel et al., 2021).

1.3 WNT Signaling

Wingless Integrase-1 (WNT) signaling is an evolutionarily well-conserved growth control pathway that is constitutively active across species where cells proliferate (Niehrs & Acebron, 2012). This complex system initiates multiple transduction steps, guiding cells for directional growth and proper tissue shaping (Schneider et al., 2015). In mammals, 19 WNT genes (Nusse & Clevers, 2017) encode lipid-modified glycoproteins that are involved in different downstream pathways. WNT signaling operates through two main pathways: canonical and non-canonical.

1.3.1 The canonical WNT pathway

The canonical WNT pathway begins with the binding of WNT ligands (mainly WNT2, WNT3, WNT3a, and WNT8a) to a receptor complex of Frizzled (FZD) and low-density lipoprotein-related protein (LRP) LRP5/6. This inhibits glycogen synthase kinase-3 (GSK3), which is part of a constitutively active destruction complex that marks β-catenin for ubiquitination and degradation. Hence, β-catenin accumulates. It is transferred to the nucleus and serves as co-factor to the transcription factor T-cell factor/Lymphoid enhancer factor (TCF/LEF), thereby inducing the transcription of WNT target genes like *c-myc, Axin2* (Acebron & Niehrs, 2016), *Osteopontin,* and *suppressor of cytokine signaling (Socs2)* (He et al., 1998).

1.3.2 The non-canonical WNT pathway

The non-canonical pathway involves at least two signaling cascades.

The planar cell polarity (PCP) pathway, initiated by WNT5a and WNT11, activates Jun-N-terminal Kinase (JNK) and RHO-associated coiled-coil-containing protein kinase 1 (ROCK) through the small GTPases RHOA and RAC1. It regulates actin cytoskeleton remodeling, altering cell adhesion, migration, and shape. Furthermore, the PCP pathway is also suggested to inhibit canonical WNT signaling.

The second cascade, calcium-dependent WNT-signaling is primarily mediated by the WNT5A and FZD2 complex (Staal et al., 2008) and activates phospholipase C through a G-protein. Phospholipase C cleaves phosphatidylinositol-4,5-bisphosphate into inositol triphosphate (IP3) and diacylglycerol (DAG), releasing intracellular calcium stores. Thereby, it activates calcineurin, CAMII kinase, and protein kinase C, ultimately leading to the transcription of nuclear factor of activated T-cells (NFAT). NFAT activation triggers skeletal rearrangement processes (Sarabia-Sanchez & Robles-Flores, 2024).

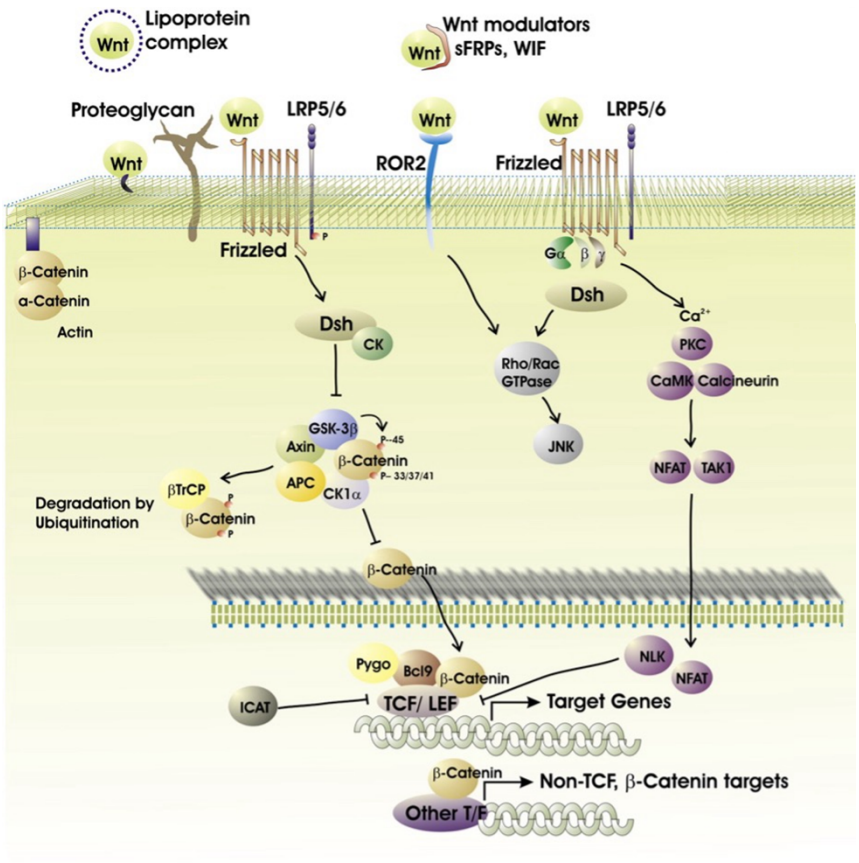

Figure 2 Overview of WNT-Signaling pathways. Modified from Malhotra et al. (Malhotra & Kincade, 2009)

1.3.3 Implications of WNT-signaling in hematopoiesis

The role of canonical WNT in adult hematopoiesis is not yet completely understood. There is evidence, that canonical WNT signaling induces self-renewal in LT-HSCs (Liu et al., 2019) and maintains the stem cell pool through WNT3a and ß-Catenin (Baba et al., 2005; Fleming et al., 2008). However, ß-

Catenin was shown to be dispensable for hematopoiesis. Moreover, long-term stabilized ß-Catenin lead to a decline of HSC numbers and induced a multilineage differentiation block (Kirstetter et al., 2006). Observations based on these differing findings imply that the physiologic effect of the canonical WNT pathway on HSCs depends not only on the cellular context but also on the extent of WNT activation as well as the presence of other variables that control canonical WNT signaling to maintain HSCs (Yu et al., 2024).

However, authors have shown the necessity of ß-Catenin to shape the hematopoietic niche (Nemeth et al., 2009), predominantly osteoblasts. Others have demonstrated that WNT inhibition in the hematopoietic niche led to activation of the canonical WNT pathway through autocrine WNT production and loss of quiescent HSCs (Schaniel et al., 2011).

Non-canonical WNT ligands, like WNT5a are expressed by HSCs, MPPs, BM stromal cells and B-lymphocytes (Liang et al., 2003). WNT5A has been shown to inhibit WNT signaling and to retain LT-HSCs in the G0 phase. A WNT5A haploinsufficient niche failed to regenerate blood in serial transplantation experiments: LSKs showed an apolar distribution of F-Actin with consequent reduction in their ability to adhere, migrate and, ultimately, home to their BM niche (Schreck et al., 2017). Furthermore, for WNT5A-treatment of LT-HSCs, but not for WNT3A, a positive long-term regulation was found (Nemeth et al., 2007).

The endosteal niche is the region, where LT-HSCs that are kept in dormancy reside. Here, they are attached to N-cad+ Osteoblasts, that, predominantly express non-canoncial WNT ligands. Thus, non-canonical WNT has a relevant role in the maintenance of LT-HSC (Sugimura et al., 2012).

1.4. The HSC supporting cell line UG261B6

One of the fundamental questions in hematologic research concerns the molecular mechanisms and conditions that control the maintenance of HSCs in the bone marrow. In previous works, Oostendorp et al. subdissected the embryonic Aorto-Gonads-Mesonephron region and established a hundred

stromal cell lines. They identified the embryonic urogenital ridge as the source of stromal cells that support hematopoietic stem cell activity most effectively (Oostendorp et al., 2002) . The UG261B6 stromal cell line, the first to maintain LT-HSCs in culture conditions for more than four weeks, was generated. When comparing the gene expression profiles of UG261B6 cells with non-supporting cell lines, Oostendorp et al found, that one-third of the genes expressed at higher levels in UG261B6 cells encoded secretory proteins (Oostendorp et al., 2005). The most upregulated genes included Pleiotropin (PTEN), Cathepsin K (CTSK), WNT5a and Secreted frizzled-related protein 1 (SFRP1) (Renstrom et al., 2009). Direct cell-cell-contact with the UG261B6 cell line was not necessary to maintain LT-HSCs, emphasizing the importance of secretory factors in the hematopoietic niche. Wöhrer et al. transplanted LT-HSC, that were previously kept in single-cell-culture on conditioned medium from UG261B6 cells and demonstrated, that, compared to several cytokine cocktails, the generation of progeny with durable self-renewal was best in cells incubated with UG261B6-conditioned medium (Wohrer et al., 2014). Also, the single cell assay proved a valuable tool to identify the biological mechanisms, by which different cytokines regulate in vitro expansion of stem cells. Thus, for example, SCF and IL-11 sustained the viability and proliferation of activated HSC, while only a cocktail containing collagen and nerve growth factor in addition to SCF and IL-11was able to promote self renewal in HSC, although to a lesser extent than UG261B6. For this work, SFRP1 and CTSK were chosen to be examined further.

1.5. SFRP1

Secreted frizzled-related Protein 1 is a family member of 5 secreted proteins in mammals that regulate WNT signaling. SFRP1 contains a cysteine rich domain that has a 30-50% homology to FZD, which inspired its name, and a C-terminal Netrin domain that binds WNTs.

Whilst early research suggested a WNT-inhibiting function, recent evidence revealed that nanomolecular concentrations of SFRP1 promote canonical WNT whereas high levels of SFRP1 induce ß-catenin degradation (Xavier et al., 2014).

Due to its WNT/ß-catenin antagonizing properties, *Sfrp1* functions as a tumor suppressor. Epigenetic silencing of *Sfrp1* has indeed been observed in a variety of cancers as well as different kinds of leukemia, whereas in other cancers, *Sfrp1* is enhanced, suggesting a context-sensitive function.

In the bone marrow niche, SFRP1 is mainly secreted by MSPCs and osteoblasts (Dufourcq et al., 2008; Nakajima et al., 2009). In *Sfrp1* $^{-/-}$ mice, Renström et al. reported increased B220^{+} B-cell populations and cycling activity in the bone marrow. Early hematopoiesis showed reduced cycling activity of MPP and LSK, although the frequency of LSK was not diminished. Whilst no intrinsic effects were shown in transplantation of *Sfrp1* $^{-/-}$ LSK into WT mice, in serial transplantations of WT-LSK into *Sfrp1* $^{-/-}$ recipients, stem cell exhaustion was found (Renstrom et al., 2009). It follows, that extrinsic SFRP1 rather than intrinsic SFRP1 is relevant for stress-response in hematopoiesis. Interestingly, in contrast to the reported WNT inhibitory functions of SFRP1, ß-Catenin levels were reduced in the LSK, MPP and CLP of *Sfrp1* $^{-/-}$ mice.

Concerning non-canonical WNT, there is evidence that Sfrp1 might inhibit WNT5a signaling, though this has not yet been demonstrated in hematopoiesis (Matsuyama et al., 2009).

1.6. CTSK

Secreted proteases cleave microenvironmental components of the bone marrow niche, such as chemokines, cytokines, and matrix components. This is crucial for the liberation of HSCs from their niche into the blood stream during hematopoietic stress (Klein et al., 2015) .

Along the stem cell rich endosteum, bone-lining osteoclasts secrete CTSK, a major bone-resorbing protease, that also cleaves essential SCF and CXCL12, suggesting a role in the selective recruitment of HSCs and their progenitors (Kollet et al., 2006). Due to its high expression in the UG261B6 cell line, our group has previously investigated the role of CTSK in hematopoiesis. Jardon-Alvarez found myeloid skewing, reduced LSK numbers, and decreased BM cellularity in CTSK-

deficient mice, while cell numbers in peripheral blood (PB) and spleen (SPL) were increased (Jardon-Alvarez, 2016). Transplantation of WT BM into CTSK-deficient recipients revealed changes in B- and T-lymphocyte numbers in both the BM and other hematopoietic organs (Hackl, 2016). Intrinsic CTSK deficiency, through transplantation of CTSK-deficient BM into WT recipients, caused reduced granulocyte numbers (Kehr, 2017).

These studies were conducted separately and at different times and therefore, have not yet been analyzed together in a comprehensive context. Part of this work aims to complete, reanalyze, and integrate the findings of previous studies into a unified context.

2. Aims and objectives

One of the most fundamental and yet unanswered questions in hematologic research is how to optimally expand hematopoietic stem cells in vitro. It is well known that in the bone marrow niche, early hematopoietic stem cells depend on factors secreted by their microenvironment. The following experiments explored the effects of extrinsic CTSK and SFRP1 on early hematopoietic stem cells. In the UG261B6 cell line, that preserves early hematopoietic stem cells and their capacity for differentiation and self-renewal exceptionally well, these secretory proteins are overexpressed.

Although raw data from various in vivo experiments with CTSK had already been collected, they had not yet been analyzed altogether. In this study, all existing raw FACS data underwent re-analysis. Additionally, the behavior of early $CD34^-$ SLAM cells in the presence and absence of both CTSK and SFRP1 was examined *in vitro* and compared with *in vivo* evidence.

As secreted factor, SFRP1 plays a crucial role in regulating the WNT signaling pathway in the hematopoietic niche. Initially proposed as canonical WNT inhibitor, evidence now suggests that it can also modulate non-canonical WNT signaling. RNA sequencing data from LSK cells regenerated in a WNT5A-haploinsufficient niche revealed several dysregulated genes associated with autophagy, endocytosis, and actin cytoskeleton regulation. To shed light on the link between SFRP1, WNT5A and canonical WNT signaling, small molecule inhibitors targeting some of these genes were identified and screened for their effects on early hematopoiesis.

3. Materials and Methods

3.1 Materials

3.1.1 Consumables

Product	Manufacturer
Cell Culture Plates Cellstar 6well	Greiner Bio-One GmbH (DE)
Cryogenic vial, 2 mL	Corning Inc. (USA)
Filter 22 µm, 30 µm, 45 µm	BDTM Filcon, BD Bioscience (DE)
Filter tips TipOne 1-10 µL, 20 - 200 µL, 200 - 1000 µL	Starlab (Hamburg, DE)
MicroAmp® Fast 96-Well Reaction Plate	Applied Biosystems (USA)
Microcentrifuge safe-lock tubes, 1.5, 2 mL	Eppendorf AG (DE)
Microplate, 96 well	Greiner Bio-One GmbH (DE)
Monoject, blunt cannula needles with Aluminium hub	Cardinal Healthcare (USA)
Polypropylene centrifuge tubes 15, 50 mL	Greiner Bio-One GmbH (DE)
Serological Pipettes, 2, 5, 10, 25, 50 mL	Greiner Bio-One GmbH (DE)
Steritop-GP, 0,22 µm, Polyethersulfon, 500 ml, 33 mm	Millipore Co. (USA)
Tissue Culture Dish, 10 mm	TPP Techno Plastic Products AG (CH)

Table 1 List of used consumables

3.1.2 Machines

Product	Name	Manufacturer
Cell sorter	MoFlo High Speed	Beckman (US)
Centrifuges	Megafuge 3.0RS Multifuge 3S Biofuge fresco Sigma 1-14	Heraeus Instruments (DE) Heraeus Instruments (DE) Heraeus Instruments (DE) Sigma Laborzentrifugen GmbH (DE)

Counting chamber	Neubauer-improved	Paul Marienfeld GmbH (DE)
Flow cytometer	CyAn ADP LxP8	Leica (DE)
Ice machine	S.-No:061244	Ziegra Eismaschinen (DE)
Incubator	Hera Cell 240	Heraeus Instruments (DE)
Laminar flow hood	ANTAES 48/72	BIOHIT (DE)
Microscope	CKX41	Olympus Corporation (Japan)
UV/Visspectrophotometer	NanoDrop ND-1000	NanoDrop Technologies (USA)
Precision scales	PLJ 2100-2M	Kern & Sohn GmbH (DE)
QuadroMACS Separator	MACS	MACS Miltenyi Biotec (DE)
Radiation Unit	Gulmay	Gulmay (USA)
Real-Time PCR System	StepOne	Applied Biosystems (USA)
Vortex	IKA MS1 minishaker	Werke & Co. (DE)

Table 2 List of used machines

3.1.3 Chemicals

Product	Manufacturer
Ethanol, 99.8 %	AppliChem (DE)
HBSS	Invitrogen (DE)
HEPES	Invitrogen (DE)
Isofluran 100 %	Abbott Laboratories (USA)
Isopropanol	Sigma-Aldrich (DE)
Propidium-Jodid (PI)	Invitrogen (DE)
Trypan blue	Invitrogen (DE)
UltraPure Dnase/Rnase-Free Distilled Water	Invitrogen (DE)

β-Mercaptoethanol	Invitrogen (DE)

Table 3 List of used Chemicals

3.1.4 Cell lines

Name	Manufacturer
UG26-1B6-pLKO.1	Oostendorp et al., 2002 Renström et al., 2009
UG26-1B6-shSfrp1	Oostendorp et al., 2002 Renström et al., 2009
UG26-1B6-shCtsk	Jardon Alvarez, Hausinger et al. 2019

Table 4 List of used cell lines

3.1.5 Biological reagents

Product	Manufacturer
Albumin Fraction V, ≥ 98 %, bovine (BSA)	Carl Roth (DE)
Fetal Calf serum	PAA (DE)
Gelatine from bovine skin	Sigma-Aldrich (DE)
Horse serum	BioWhittaker (DK)
LDL, human	Stemcell Technologies (DE)
Penicillin/Streptomycin	Invitrogen (DE)
Puromycin	Invitrogen (DE)
Trypsin 10x	Invitrogen (DE)

Table 5 List of used Biological reagents

3.1.6 Ordered buffers, media and solutions

Product	Manufacturer
α-MEM plus GlutaMAX	Inivtrogen (DE)
BIT 9500 Serum Substitute	Stemcell Technologies (DE)

Dulbecco's Modified Eagle Medium (DMEM)	Invitrogen (DE)
Dulbecco's phosphate buffered saline (DPBS)	PAA (DE)
Hank's Buffered Salt Solution, 10x (HBSS)	Invitrogen (DE)
HEPES	Invitrogen (DE)
Iscove's Modified Dulbecco's Medium (IMDM)	Thermo Fisher Scientific Inc. (USA)

Table 6 List of ordered buffers, media and solutions

3.1.7 Self-made buffers, media and solutions

Name	Composition
FACS buffer	500 ml PBS 5% BSA
Freeze medium	90% heat-inactivated calf serum, freshly thawed 10% Dimethyl sulfoxide
Gelatin	0.4 g gelatin powder 400ml distilled H_2O → autoclaved in a loose-cap 500ml glass bottle
HF2 buffer	86% distilled H_2O 10% HBSS (10x) 2% heat-inactivated fetal calf serum 0.1% HEPES 100 U/ml penicillin 100 mg/ml streptomycin → mixed well and filtered through a 0.22µm bottle-top filter
Stroma medium	α-MEM plus GlutaMAX 15% heat-inactivated fetal calf serum 5% heat-inactivated horse serum 100 U/ml penicillin 100 mg/ml streptomycin 10 mM ß-Mercaptoethanol → mixed well and filtered through a 0.22µm bottle-top filter

Trypsin	45 ml PBS 5 ml Trypsin 10x

Table 7 List of self-made buffers, media and solutions

3.1.8 Kits

Product	Manufacturer
FITC Annexin V Apoptosis Detection Kit I	BD Pharming (USA)
Lineage cell depletion kit, mouse	Miltenyi Biotec (DE)
Power SYBR Green PCR Master Mix	Applied Biosystems (USA)
Quanti Tect Reverse Transcription Kit	Qiagen Inc. (DE)
RNeasy Mini Kit	Qiagen Inc. (DE)

Table 8 List of used Kits

3.1.9 Antibodies

Antigen	Fluorochrome	Volume	Clone	Company
Anti-mouse CD3e	PE-Cy5.5	0.1 µl	145-2C11	ebioscience (USA)
Anti-mouse CD4	PE-Cy5.5	0.1 µl	30-F11	ebioscience (USA)
Anti-mouse CD8a	PE-Cy5.5	0.1 µl	53-6.7	ebioscience (USA)
Anti-mouse CD11b	APC APC-eFluor®780	0.1 µl	M1/70	ebioscience (USA)
Anti-mouse CD34	FITC	0.1 µl	RAM34	ebioscience (USA)
Anti-mouse CD45	FITC PE PE-Cy5.5. PE-Cy7 eFluor®450 APC APC-eFluor®780	0.1 µl	30-F11	ebioscience (USA)
Anti-mouse CD45R (B220)	PE-Cy7 PE-Cy5.5	0.1 µl	RA3-6B2	ebioscience (USA)
Anti-mouse CD117 (KIT)	APC PE	0.1 µl	2B8	ebioscience (USA)
Anti-mouse CD150	APC PE	0.1 µl	9D1	ebioscience (USA)
Anti-mouse Gr-1 (Ly-6G)	eFlour450®	0.1 µl	RB6-8C5	ebioscience (USA)
Anti-mouse SCA-1	PE PE-Cy7	0.1 µl	D7	ebioscience (USA)
Biotinylated anti-mouse CD3e	-	0.1 µl	145-2C11	ebioscience (USA)
Biotinylated anti-mouse CD11b	-	0.1 µl	M1/70	ebioscience (USA)
Biotinylated anti-mouse CD48	-	0.1 µl	HM48-1	ebioscience (USA)
Biotinylated anti-mouse B220	-	0.1 µl	RA3-6B2	ebioscience (USA)
Biotinylated anti-mouse Gr1 (Ly-6G)	-	0.1 µl	RB6-8C5	ebioscience (USA)

Biotinylated anti-mouse TER-119	-	0.1 µl	TER-119	ebioscience (USA)
Streptavidin secondary antibody	eFluor450®	0.1 µl	-	Invitrogen (DE)

Table 9 List of used antibodies

3.1.10 Primers

Primer name	Sequence 5'→ 3'
CTSK2 forw	CTCCCAGTGGGTGTCCAGTATC
CTSK2 rev	GCTCAAGGTTCTGCTGCTACCT
CTSKR3 forw	CCAGTGGGAGCTATGGAAGA
CTSKR3 rev	AAGTGGTTCATGGCCAGTTC
Rpl39 F	ATTCCTCCGCCATCGTGCGCG
Rpl39 R	TCCGGATCCACTGAGGAATAGGGCG
***Sfrp1*-F**	AATCCAGTCGGCTTGTTCTT
***Sfrp1*-R**	CTAATCTAAATGGCCCTTGCTTTAC

Table 10 List of used primers

3.1.11 Mice strains

Name	Manufacturer
C57/BL6.J	Harlan Laboratories (DE)
129x C57/BL6.J	Breeding in ZPF: 129S2/SvHsd x C57/BL6.J

Table 11 List of used mice strains

3.1.12 Software

Name	Manufacturer
Graphpad Prism 10	GraphPad Software, Inc (USA)
Snapgene	GSL Biotech LL (USA)
Stepone™ Software v2.2	Applied Biosystems (USA)

Table 12 List of used software

3.1.13 Inhibitors

Name	Inhibits	Manufacturer
SecinH3	Cyth1/Cyth2	Tocris (UK)
Spautin-1	BECN1	Sigma-Aldrich (GE)
CPYPP	DOCK2	Tocris (UK)
ISA2011B	Pip5k1a	gift
Edelfosine	PLC	Sigma-Aldrich (GE)

Table 13 List of used inhibitors

3.2 Methods

3.2.1 UG261B6 cell line and its maintenance

In the aorta-gonads-mesonephros (AGM) region, the first repopulating hematopoietic stem cells originate in the murine embryo. Increasing activity of HSCs is found in the urogenital ridge of the midgestational embryo between day 10.5 and 11. Oostendorp et. al found that stromal clones derived from the urogenital subregion of the AGM support HSC survival in vitro exceptionally well compared to other AGM subregions or adult bone marrow stromal cells (Oostendorp et al., 2002).

The abovementioned stromal cell line was created in 2002 and is derived of the urogenital ridge of transgenic mouse lines expressing the thermolabile tsA58 gene, which is a commonly used immortalizing gene to generate cell lines.

Although lentiviral knockdown experiments are regularly conducted within our research group, the knockdowns discussed in this study were already existent. To ensure the stability of the knockdown, cells were treated with puromycin. Thawed UG261B6 knockdowns were washed and cultured in stroma medium containing 5mg/ml puromycin on 0.1% gelatine-coated dishes at 33°C with 5% CO2 and >95% humidity. Following exposure to puromycin, only successfully transduced cells containing the integrated puromycin resistance gene within the expression cassette would survive. It was avoided to grow the cells to confluency to prevent contact inhibition and senescence.

For harvesting, the culture medium was aspirated, cells were washed gently with PBS to remove residual medium or cell debris. The cells were then incubated with 0,5% trypsin solution for 5 minutes. Detachment of the cells was checked under the microscope, then they were aspirated and transferred to a sterile tube containing stroma medium to neutralize the trypsin. Cells were spun down at 300g and resuspended with 1ml stroma medium for counting. 20µl of viable cells was stained with 20µl 0.4% trypan blue and counted under the microscope using a

Neubauer hemocytometer. The result was multiplied by 10^4 x ml to obtain the final cell number.

Then, cells were either replated on coated dishes, reaching their next passage, or resuspended in freeze medium and frozen at -80°C or transferred in an RNase free tube and used for RNA isolation. For experiments, controls and knockdowns from the same passages were used.

3.2.2 RNA isolation, reverse transcription and real-time qPCR

Verification of the knockdowns was performed by analysis of the specific gene expression levels of *Sfrp1* and *Ctsk* using quantitative real-time polymerase chain reaction (RT-qPCR). RT-qPCR is a method for amplification and quantification of a specific RNA molecule and a reference gene. The reference gene, that is constitutively expressed in the cell concerned, serves as an internal control to which the expression level of the target gene is later normalized.

Extraction and purification of total RNA

To obtain total RNA, the frozen cell pellet first needs to be lysed and subsequently, the RNA is extracted and further purified. This was done with the RNeasy Mini Kit from Qiagen, according to the manufacturer's instructions. Initially, cells were lysed with 350µl of a guanidine thiocyanate-containing lysis buffer (RLT Buffer), that disrupts cellular structures, and 10µl of ß-mercaptoethanol to inactivate RNases. mechanical disruption was additionally performed through vortexing. For homogenization, the lysate was transferred into a QIA shredder spin column and centrifuged at full speed, the flow-through was caught in a collection tube.

1 volume of 70% ethanol was then added to the sample. Ethanol and guanidine thiocyanate both facilitate the binding of RNA to a silica membrane. The lysate was then applied to the silica membrane (RNeasy spin column) and centrifuged for 15 second’s maximum speed. DNA, salts, proteins and other cellular components were removed through repeated washing, yielding purified RNA. Initially, 700µl of ethanol-containing RW1 buffer was used for washing, then

repeated washes with 500 µl of concentrated RPE buffer were performed. Remaining wash buffer was removed by centrifugation of the membrane for 1 minute at full speed.

Finally, by adding 50µl of RNase-free water directly onto the spin column, the RNA was eluted into a new collection tube. The sample was spun down at full speed. To prevent degradation, the purified RNA was afterwards kept on ice.

The RNA amount of each sample was then quantified by measuring the optical density at 260/280nm using a spectrophotometer. The RNA was then aliquoted and stored at -80°C.

Primer design for RT-qPCR

The target mRNA sequence was obtained from the UCSC Genome Browser. As primer binding sites, exons that had a minimum base pair length of 1000bp and were conserved within the mRNA sequence were selected.

The nucleotide sequence was then inserted into the primer design tool Primer3. The following criteria were set: Primer length: 18-22 base pairs, product size: 80-120 base pairs, melting temperature: 60 ±2°C. From the proposed primers, those with a GC-content between 40-60% and that had no inter- or intra-primer homology were selected.

To evaluate for primer specificity, binding sites and amplicon length, the primer sequence was analyzed with SnapGene. SnapGene is a software tool for the visualization and analysis of DNA sequences. Subsequently, the primers were ordered from Thermofisher.

To assess primer performance, a serial dilution with known concentrations of universal mouse DNA was used. The PCR master mix, that is described further below, was added, and real-time quantitative PCR (RT-qPCR) was performed. The read-out of the RT-qPCR consisted of a standard curve, where threshold cycle (CT) – values were plotted against the DNA concentrations. By Linear

regression analysis using Microsoft Excel, the coefficient of determination, R^2 was obtained. Primers with an R^2 value of >0.9 were considered appropriate, which indicates high PCR efficiency.

Reverse transcription of total RNA into complementary DNA (cDNA)

Reverse transcription from RNA to complementary DNA (cDNA) was performed using the QuantiTect Reverse Transcription Kit from Qiagen. Reverse transcriptase is a multifunctional enzyme. It's RNA-dependent DNA-Polymerase activity catalyzes the transcription of the RNA-template into cDNA. The RNase H activity of the enzyme specifically degrades the RNA in RNA-DNA hybrids without affecting pure RNA.

First, 2µl of genomic DNA wipeout buffer as well as a variable amount of water was added to the RNA until a total reaction volume of 14µl was achieved. If more than 1µg RNA was used, the reaction volume was scaled up. The mix was incubated for 2 minutes at 42°C, afterwards kept on ice. Then, a reverse transcription master mix with 1µl Quantiscript reverse transcriptase enzyme, 4µl Quantiscript RT Buffer nucleotides, and 1µl Primer Mix of random primers was applied to the sample. After 15 minutes of incubation at 42°C, the enzyme reaction was terminated by heating the sample up to 95°C.

Real-time Polymerase Chain Reaction

RT-qPCR was carried out with the StepOnePlus Real-Time PCR System with the fluorescent dye Power SYBR Green PCR Master Mix (Applied Biosystems). A RT-qPCR machine on one hand performs a process called thermal cycling to synthetize double-stranded DNA (dsDNA) and on the other hand simultaneously detects fluorescence that is emitted when dsDNA is produced.

In the first step of RT-qPCR, the DNA is denaturated into single strands at a high temperature of 95°C. Then, the temperature is lowered to approximately 55°C, where the primers can anneal to the single-stranded DNA. During extension phase at 70°C, the DNA polymerase reaches its optimal operating temperature

and synthetizes DNA by elongation of the annealed primers. This cycle of denaturation, annealing and extension is repeated approximately 40 times. During extension, the fluorescent SYBR Green intercalates dsDNA and through interaction with the DNA molecule, emits a higher fluorescence. The more dsDNA is produced, the more fluorescence is emitted. The detected amount of fluorescence is directly proportional to the amount of DNA molecules at each cycle during DNA amplification. Besides the fluorescent dye, the SYBR Green PCR master mix contains DNA polymerase, dNTPs and magnesium.

The PCR master mix composition as follows:

Forward primer	0.05µl
Reverse primer	0.05µl
cDNA	1µl
H_2O	8.9µl
SYBR Green	10µl
Total volume per well	**20 µl**

Table 14 RT-PCR mastermix

The reaction components were mixed by flicking the tubes and then centrifuged to collect contents at the bottom of the tube. The plates were loaded with triplicates of each sample and with a no-template control (to test for contaminations and primer dimers), and then sealed with an optical cover. To reduce entrapment of air bubbles through pipetting and collect sample adhering to the walls of each well, plates were centrifuged, then inserted into the thermal cycling block and the RT-qPCR run started.

Phase	Temperature	Time	
Denaturation	50 °C	5 min	
Annealing	95 °C	15 sec	40 cycles
Extension	58 °C	30 sec	
Hold	4 °C	unlimited	

Table 15 RT-PCR protocol

Success of DNA amplification PCR product was analyzed. Therefore, the amplification and melting curves were examined. An adequate amplification curve was considered sigmoidal: as the amount of fluorescence mirrors the amount of dsDNA, at the beginning of the RT-qPCR there is little target DNA. It follows an

exponential phase with a rapid increase in target DNA. The limitation in reagents leads to a reaction plateau, then it finally stagnates. Specificity of the DNA product was assumed when the melting curve showed a single, well defined melting peak with sharp decrease.

The CT value of the reference gene was subtracted from the CT value of the target gene to obtain the ΔCT value.

3.2.3 Generation of serum-free conditioned medium

Stromal cells were grown to 90% confluency on 10cm dishes and immortalized by irradiation with 30gy. After the stroma medium was discarded, three wash steps were performed with PBS to remove residual serum from culture media. Serum free culture medium BIT 9500 Serum Substitute was diluted with IMDM to a final concentration of 20% and supplemented with Penicillin/Streptomycin (100U/ml and 100mg/ml), low density lipoproteins (40mg/ml) and ß-mercaptoethanol (1:1000). 12ml of the master mix were added onto the 10cm dish and conditioned for 3 days at 33°C with 5% CO2. The conditioned medium was then collected and filtered through a 30µm syringe filter (Whatman).

When working with small molecule inhibitors, they were added on the day of the cell sort before filtering the solution. The control media were substituted with the same amount of DMSO as used for restitution of each inhibitor. The maximal DMSO concentration was 1:3000 to prevent an influence of DMSO itself on the cells.

3.2.4 Reconstitution and titration of small molecule inhibitors

An extensive literature review was performed to determine the optimal concentration range for each small molecule inhibitor. Inhibitors were selected for which IC50 values had already been published. Data on IC50 for cell culture experiments were preferred. When information was available only for in vivo experiments, we used the data related to mouse experiments. First, the inhibitor at the published IC50 and at concentrations three times lower and higher was

tested. The concentration range was step by step adjusted based on the oberserved effects.

The MTT assay was not practical for the experimental setting that examined the rare population of LT-HSCs. The MTT assay requires a high number of cells to achieve an acceptable seeding density (e.g., 5000 cells per well on a 96-well plate) compared to the 60 cells needed for one 96-well plate for the single-cell essay. We focused our investigations on evaluating the effects of inhibitors on proliferation, differentiation, and apoptosis. The inhibitors were reconstituted with DMSO and stored following the manufacturer's instructions.

To minimize the cytotoxic effects of DMSO, we avoided using concentrations higher than 0.1%. Therefore, when necessary, the inhibitors were prediluted in serum-free conditioned medium immediately before use.

3.2.5 Mice and preparation of murine tissue

129x Ly5.1 mice were used as stem cell donors. The animals were kept according to the Federation of Laboratory Animal Science Associations and institutional guidelines. The animal experiments were approved by the Government of Upper Bavaria (Hausinger et al., 2021).

For bone marrow experiments, 6-8 weeks old mice were sacrificed. Femora and tibiae were cut at the ends, and bone marrow was flushed out and resuspended with a blunt needle in ice cold HF2 buffer. The suspension was then passed through a 30µm syringe filter and centrifuged at 500 rpm for 5 minutes.

Lineage separation was performed with the lineage separation kit from Miltenyi according to the manufacturer's instructions. The cell suspension was stained with a primary monoclonal anti-biotin antibody against the lineage marker CD34 and incubated on ice for 10 minutes, then cells were washed with HF2- buffer. The secondary labelling was done with biotinylated magnetic beads (MicroBeads) for 15 minutes on ice. A MACS column was then attached to the MACS separator which produces a magnetic field and equilibrated with HF2 buffer. Cells were then

applied to the column which retained the $CD34^+$ cells. The columns were rinsed three times to increase the yield of the lineage negative population. Then, the MACS columns were removed from the MACS separator to interrupt the magnetic field and the lineage positive cells were flushed out in separate tubes. They were used as single stains for the cell sort.

3.2.6 Flow Cytometry and cell sorting

$CD34^-$SLAM cells were isolated from the previously lineage-depleted BMby antibody staining of their surface markers and cell sorting. The staining was performed in a total reaction volume of 100µl/5 mice in $HF2^+$ buffer in the dark on ice, cells were incubated for 60min, then washed with $HF2^+$. The antibodies are listed in **Table 9**. The bone marrow staining protocol for cell sort of $CD34^-$ SLAM cells:

Lineage panel: CD3e, GR1, Ter119, B220, CD11b, CD48 + Streptavidin 0,5µl/10^6 cells – PECY 5.5 (secondary)

CD48-PECy5.5 3µl/10^6 cells

Ckit-APC 3µl/10^6 cells

Sca1-PECy7 3µl/10^6 cells

CD34-FITC 2µl/10^6 cells

CD150-PE 3µl/10^6 cells

Using a MoFlo High Speed cell sorter, we first removed doublets by gating on forward scatter (FS) and pulse width (PW). In the gate for sideward scatter (SS)/FS, we used size and granularity to differentiate between cells and debris. Next, we enriched for living cells by selecting the PI-low population via gating for PI/forward scatter. Then, we gated for c-kit, a marker typical of hematopoietic stem cells and myeloid progenitors, and lineage-negativity (B220, CD3e, CD11b, CD48, Gr1, TER119) to further refine the population. Finally, we used Sca-1,

also a marker for early HSCs and progenitors, gated against c-kit to isolate the LSKs.

$CD34^-$SLAM cells are the most primitive HSCs able to generate all types of blood cells. They can be identified by high expression of CD150. To isolate them, the LSKs were sorted based on CD150 and CD34 expression. The resulting population was $CD34^-$, $CD48^-$, $CD150^+$, $SCA\text{-}1^+$, KIT^+ LSK, also known as $CD34^-$SLAM cells.

3.2.7 Single cell assay

On the day of cell sorting, stem cell factor (100 ng/ml) and IL-11 (20 ng/ml) were added to the conditioned medium. Round-bottomed 96-well plates were preloaded with 94 µl of medium and stored at 37°C until sorting.

A single $CD34^-$ SLAM cell was sorted into 60 wells of a 96-well plate containing conditioned medium, the rest of the wells was filled with 200µl distilled water to prevent drying out, the plates were centrifuged at 300 rpm for 2 minutes without brakes to center the cells in the round-bottom plate. Thus, they could easier be localized under the light microscope.

Plates were inspected daily (around the same time) for growth under a light microscope, starting 24 hours after sorting, for 5-7 days. Cells were then harvested and analyzed with flow cytometry for differentiation and apoptosis.

The staining protocol for the differentiation panel can be found below. Cells were incubated for at least 30min in the dark on ice and washed with HF2.

Bone marrow Staining for Differentiation- FACS:

Gr-1-PB/55 µl/10^6 cells

cKit-PE/5 µl/10^6 cells

Sca1-PECy7/5 µl/10^6 cells

B220 + CD3e-PECy5.5/5 µl/10^6 cells

CD11b-APC/5 µl/10^6 cells

Apoptosis was examined using Annexin-V-staining with the FITC Annexin V Apoptosis Detection Kit I (BS Pharming). This method works since processes that occur in the cell membrane when cells enter apoptosis. First, a cell pellet of 10^5 cells is resuspended in 500µl of Annexin buffer. 5 µl of Annexin conjugated to the fluorescent dye FITC and 10µl propidium iodide are added to the sample, vortexed and incubated on ice for 15 minutes, then fluorescence is measured within one hour. Annexin V binds to phosphatidylserine, which is a part of the cell membrane and usually kept inside the cell, where it is not accessible for Annexin V. When a cell enters apoptosis, phosphatidylserine is exposed on the outer surface and hence can be bound by Annexin V. The emitted fluorescence therefore detects phosphatidylserine and is a measure for early apoptosis. Propidium iodide is a fluorescent dye that intercalates DNA but cannot enter cells with an intact cell membrane. During late apoptosis, the cell membrane is compromised. Cells that are PI positive, are therefore in a stage of late apoptosis.

It follows, that cells that are Annexin V negative and PI negative, are alive. Annexin positive but PI negative cells have entered early apoptotic stage and cells positive for both Annexin V and PI are considered necrotic.

3.2.8 Analysis of single cell assays

For Clone size, the cells were daily counted under the microscope. It was defined as the number of viable cells per well on each day of observation. Survival was the presence of one or more cells in each well. Time to first division was the day when more than one cell was first observed in a well. Additionally, the percentage of wells with divided cells, i.e., those with more than two cells, was calculated.

3.2.9. Statistical analysis

GraphPad Prism 7 was used to perform the statistical analyses. Were unlcear, normal distribution was analyzed with the Kolmogorov-Smirnov test. The level of significance was explored with the nonparametric Mann-Whithney test, as the data were not normally distribbuted. When comparisons of more than two groups were needed, the one-way analysis of variance test was used. Dunnett's multiple comparison test was then applied as post hoc test. Statistical significance was assumed whith a p value < 0.05. The data were visualized as dot plots with means $\pm$ systematic error of the mean (Hausinger et al., 2021).

4. Results

To identify the factors that influence the maintenance, proliferation, differentiation, and survival of hematopoietic stem cells in vitro, single cell experiments were conducted. Single CD34^{-} SLAM cells were therefore cultured in conditioned, serum-free media from the cell line UG261B6. The non-contact nature of this setup is essential to eliminate potential cell-cell interactions.

This thesis investigates two secreted factors within the hematopoietic niche: SFRP1 and CTSK. It's noteworthy that neither of these factors is expressed by hematopoietic stem cells (HSCs); they are produced by stromal and osteogenic cells. The in vitro findings are then compared with existing data from in vivo experiments.

4.1 Characteristics of CD34- LSKS cultured in single cell cultures in the presence or absence of CTSK

Secreted CTSK cleaves Collagen and promotes HSC release from the bone marrow niche. Therefore, we proposed that absence of CTSK would dysregulate HSC function and expansion in vitro.

To investigate the extrinsic effects of CTSK on HSCs in vitro, we utilized existing *Ctsk* knockdowns from the UG26-1B6 cell line, with the corresponding empty vector control. The cells were thawed and plated onto gelatine-coated dishes and cultivated to confluence. Puromycin was substituted to select clones with intact *Ctsk* knockdown. Cells were harvested, RNA was isolated, and cDNA was synthesized for qPCR confirmation of the downregulation of *Ctsk* (**Fig. 3A**).

Following verification of the knockdowns, we generated serum-free conditioned medium (**see Methods, 3.2.3**). For the single-cell experiments, we isolated CD34$^-$ SLAM cells from the murine bone marrow. A single cell was sorted into 96-well round-bottomed plates preloaded with serum-free conditioned medium from either UG26-1B6 *pLKO.1* or sh*Ctsk2* and sh*Ctsk4.* The conditioned medium was

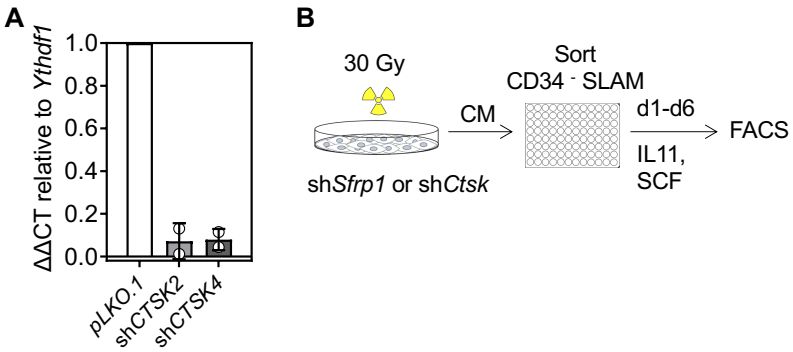

Figure 3 Generation of knock-down stromal cell lines and experimental design for single cell assay

A mRNA content of *CTSK with Ythdf1* as housekeeping gene in the UG26-1B6 knockdown clones *shCtsk2, shCtsk4* and the empty vector control *pLKO.1* measured by real-time-PCR. Mean down regulation from 2 experiments each: 92.84% for sh*Ctsk2*, 92.07% for sh*Ctsk4*
B Single cell assay: Conditioned medium was generated by irradiation of confluent 10cm dishes of the UG26-1B6 knockdown clones and the empty vector controls. Bone marrow was isolated and CD34- SLAM cells were enriched by FACS as described. One single cell per well was sorted into a 96 well plate with conditioned medium supplemented with SCF and IL-11. Cell number was microscopically assessed every 24h. After 6 days, the clones were harvested, stained and analyzed with flow cytometry for differentiation.

substituted with stem cell factor (SCF) and interleukin 11 (IL-11) **(Fig. 3B).** The plates were daily evaluated microscopically**.** Thereafter, the cells were harvested and analyzed by flow cytometry for differentiation and apoptosis (**Fig. 3B).**

A significant decrease of cell proliferation and clone size of CD34$^-$ SLAM cells cultured in a CTSK-deficient environment was observable from day 3 onwards (**Fig 4A**). We hypothesized, that this reduction could be due to either slower division rates or increased cell death. However, the time to the first cell division was not different between the cultures (**Fig. 4B**), suggesting cell cycle recruitment was unimpaired. Furthermore, the percentage of wells containing at least two cells on days 1 to 6 did not show significant discrepancies (**Fig. 4C**).

Regarding cell survival, we observed that from the second day onwards, 80.83-91.25% of the wells contained at least one cell in all cultures. Survival remained unchanged in HSCs cultured in sh*Ctsk2* and s*hCtsk4* versus p*LKO.1*-conditioned medium (**Fig. 4D**). We established additional cell cultures and the fractions of living, apoptotic, and necrotic cells 48 hours after culture with an Annexin V assay. As we found similar rates of cell death and apoptosis, impaired survival was not responsible for the smaller clone size (**Fig. 4E**).

Although cell cycle recruitment remained unaltered, the absence of soluble CTSK led to decreased mitogenic activity of $CD34^-$ LSK.

Regarding differentiation, we observed no severe alterations, but a trend towards myeloid skewing (**Fig. 4C**).

Our in-vitro experiments show a reduced capacity for CD34-LSK regeneration in an environment lacking CTSK. Mature hematopoiesis is unaffected.

To further contextualize our findings, we compared them with in vivo evidence. *Ctsk*$^{-/-}$ mice have previously been characterized in our research group, but until date, the experiments have not completely been analyzed together in a comprehensive context. The methodological aspects of these experiments have been described and the experiments performed by others in their respective doctoral theses (Hackl, 2016; Jardon-Alvarez, 2016; Kehr, 2017) and are therefore beyond the scope of this thesis.

In the following, we re-analyzed and interpreted all flow cytometric data from these experiments to relate them to the current work and understand the in vivo and in

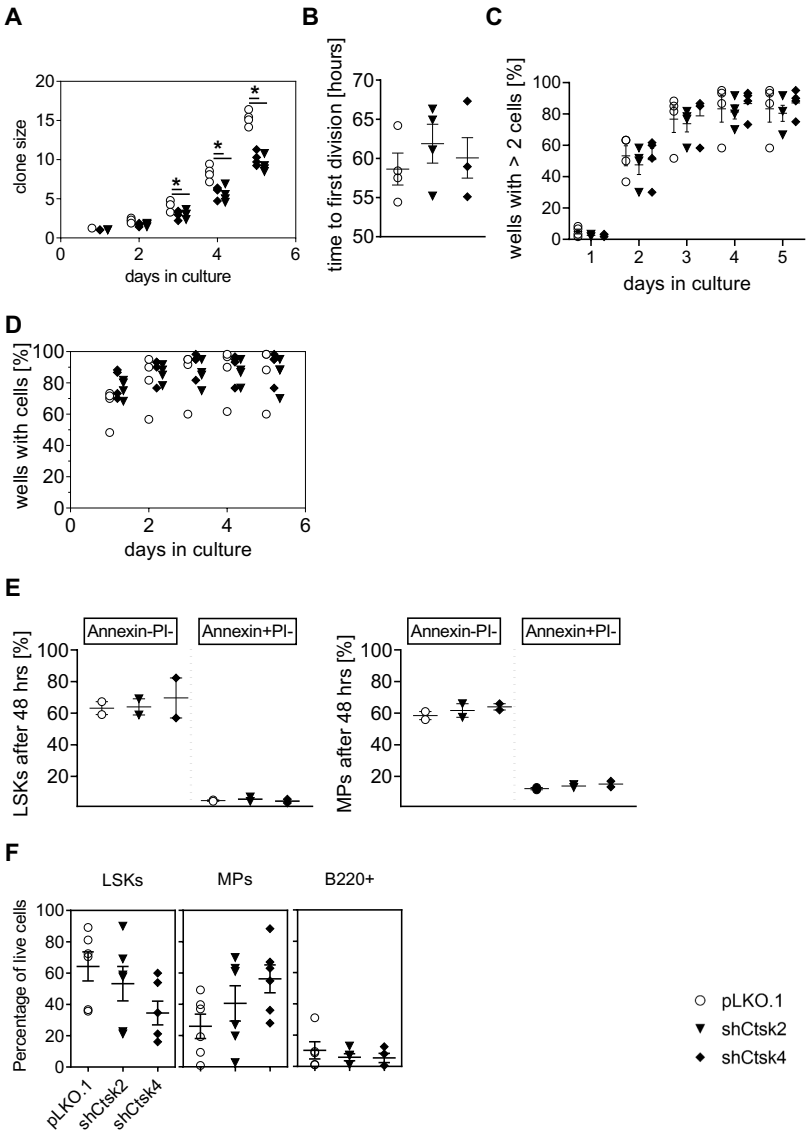

Figure 4 Proliferation, survival, cell division rate, differentiation and of single CD34- SLAM cells on CTSK deficient medium

A Microscopically evaluated mean clone size of CD34- SLAM cells cultured in p*LKO.1* or sh*Ctsk* conditioned medium. $p<0.01$ for days 3,4 and 5.
B Mean hours elapsed from spotting more than 1 cell in each well, for pLKO.1: 58.64±2.04 hrs, sh*Ctsk2*: 61.87±2.48 hrs, sh*Ctsk4*: 60.06±2.57 hrs.
C Percentage of wells with more than two cells 6 days after culture.
D Percentage of wells with detectable cells during each day of culture
E Percentage of live ($Annexin^{-}PI^{-}$) and apoptotic ($Annexin^{+}PI^{-}$) LSKs and MPs after 2 days culture
F Percentage of LSKs, Myeloid Progenitors and B220+ cells 6 days after culture

vitro effects of secreted factors on HSCs. These new data are presented in the following section.

4.2 Characteristics of Ctsk$^{-/-}$ mice

The Ctsk-deficient mice (*Ctsk*$^{-/-}$) showed no disparities in early hematopoiesis under steady-state conditions in our re-analysis of FACS data from mice aged 8-10 weeks (**Fig. 5A and 5B**). However, we found variations in lymphopoiesis across different hematopoietic tissues in *Ctsk*$^{-/-}$ mice when compared to their wildtype (WT) counterparts (**Fig. 5C-F**). We observed an increase in the fractions of CD45R+ B-lymphocytes in the peripheral blood (PB) and higher numbers of thymic B- and T-lymphocytes (**Fig. 5D, 5E**). In the small T-lymphocyte bone marrow (BM) compartment, we found a reduction in the CD3ε+ T-lymphocytes (**Fig. 5A, 45E**). In spleens (SPL) of *Ctsk*$^{-/-}$ mice, we did not find alterations of B- and T- lymphocytes.

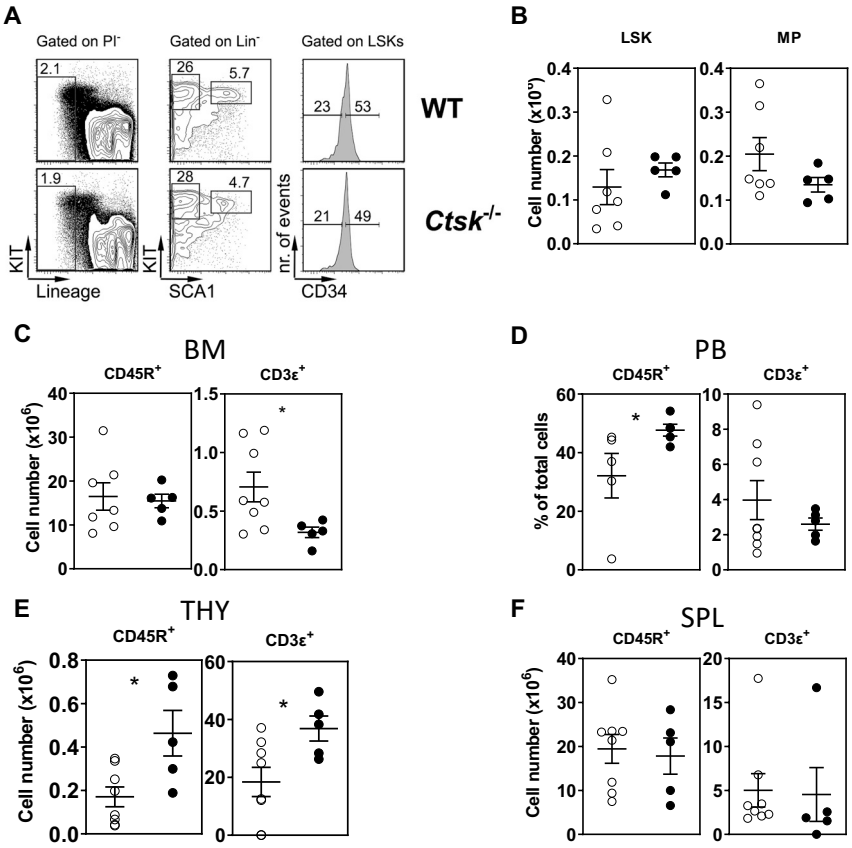

Figure 5 Effects of Ctsk loss on steady- state hematopoiesis.

A Representative contour plots of the BM stem and progenitor cells from the BM of WT and Ctsk$^{-/-}$ mice.
B Absolute numbers of CD34− LSK cells and myeloid progenitors and in the BM of WT and Ctsk$^{-/-}$ mice.
C Absolute numbers of B and T lymphocytes in the BM (CD3ε+: $70.5 \pm 12.6 \times 10^4$ for WT compared to $31.8 \pm 4.4 \times 10^4$ for Ctsk$^{-/-}$ mice, $p = .045$
D Percentages of B and T lymphocytes in the PB (CD45R$^+$: $32.1 \pm 7.6\%$ for WT, compared to $48.3 \pm 2.0\%$ for Ctsk$^{-/-}$ mice, $p \leq .032$)
E absolute numbers of B and T Lymphocytes in the THY ($17.1 \pm 0.1 \times 10^4$ for WT controls compared to $46.4 \pm 0.1 \times 104$ for Ctsk−/− mice, $p < .014$, CD3ε+: $18.4 \pm 5.1 \times 10^6$ for WT, compared to $36.8 \pm 4.3 \times 10^6$ for Ctsk$^{-/-}$ mice, $p = .045$) and **F** SPL
Closed white circles represent WT cells, closed black circles represent Ctsk$^{-/-}$ cells.

It follows that CTSK may play a regulatory role in the distribution of B and T-lymphocytes within different hematopoietic tissues.

4.3 Engraftment of wildtype hematopoietic stem cells in a CTSK deficient stromal niche

Next, we investigated the impact of a Ctsk$^{-/-}$ microenvironment on the stress response of wildtype HSCs. In this experiment, wildtype HSCs had been transplanted into lethally irradiated Ctsk$^{-/-}$ mice (**Fig. 6A**). Unexpectedly, when compared to the in-vitro data, the transplantation of wildtype HSCs into *Ctsk*$^{-/-}$ mice did not result in any impairment of overall engraftment in the PB (**Fig. 6B**) or BM (**Fig. 6C-D**). It did neither affect the engraftment of early hematopoietic cells, compared to the WT controls (**Fig. 6C- D**). However, CD45R^{+} B-lymphocytes in the BM were reduced in the BM and simultaneously, the numbers of B-lymphocytes within the thymuses (THY) were increased (**Fig. 6F-H**).

Furthermore, there were fewer CD3ε^{+} T-lymphocytes in the BM and they were strongly reduced in the SPL compared to a microenvironment with sufficient CTSK **(Fig. 6F-G)**. These findings suggest that the presence of CTSK in the microenvironment plays a regulatory role in optimizing the regeneration of donor lymphopoiesis.

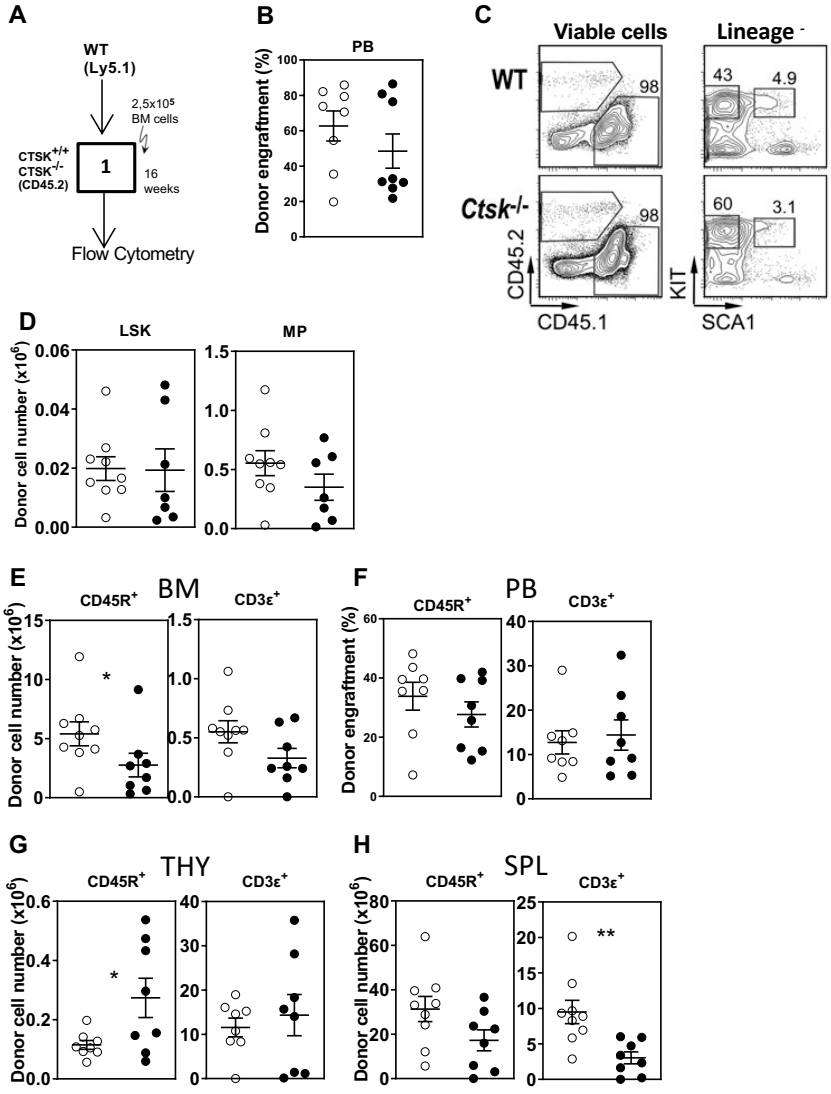

Figure 6 Role of extrinsic CTSK for regeneration of WT HSCs

A Experimental design. WT Lin$^-$ cells from congenic CD45.1 mice were transplanted into primary (1°) CD45.2 *Ctsk*$^{-/-}$ mice and WT mice. Donor cells were analyzed 16 weeks post transplantation.
B Representative contour plots of the BM stem and progenitor cells
C Percentage of donor engraftment in the PB
D Absolute numbers of CD34$^-$ LSKs and MPs in the BM of transplanted mice
E Percentage of B and T lymphocytes in the PB, absolute numbers of B and T lymphocytes in the F BM (CD45R$^+$: 5.4 ± 1.0 × 10^6 for WT compared to 2.8 ± 1.0 × 10^6 for *Ctsk*$^{-/-}$ recipient mice, p = .036), G SPL (CD3ε$^+$: 9.5 ± 1.7 × 10^6 for WT recipients compared to 3.0 ± 0.8 × 10^5 for *Ctsk*$^{-/-}$ recipient mice, p < .003)
and **H** THY (CD3ε$^+$: 11.4 ± 1.5 × 10^6 for WT recipients compared to 27.3 ± 6.6 × 10^6 for *Ctsk*$^{-/-}$ recipient mice, p < .035) of transplanted mice
Closed white circles represent WT cells, closed black circles represent Ctsk$^{-/-}$ *cells.*

4.4 Engraftment of *Ctsk*$^{-/-}$ hematopoietic stem cells in a wildtype bone marrow niche

The observed lymphocyte-regulation could be through cell-extrinsic effects, primarily via secretion of CTSK by e.g. stromal cells. However, CTSK could also be secreted by the HSC itself or, particularly, by its osteoclast progeny. In a second transplantation experiment, the impact of autocrine CTSK on hematopoiesis was assessed. Here, HSCs from *Ctsk*$^{-/-}$ mice were transplanted into WT mice. Total PB cells repopulated poorly in the absence of CTSK (**Fig. 7A-B**). As the engraftment of early hematopoietic donor cells in the BM was unimpaired, altered myelopoiesis was not responsible for poor repopulation (**Fig. 7B-C**). Interestingly, only the absolute numbers of CD3ε+ T-lymphocytes in the BM were reduced, a finding that was seen before in steady state hematopoiesis and extrinsic transplantation (**Fig. 7D**). The SPL and PB as peripheral lymphocytic compartments showed unaltered engraftment of donor-lymphocytes.

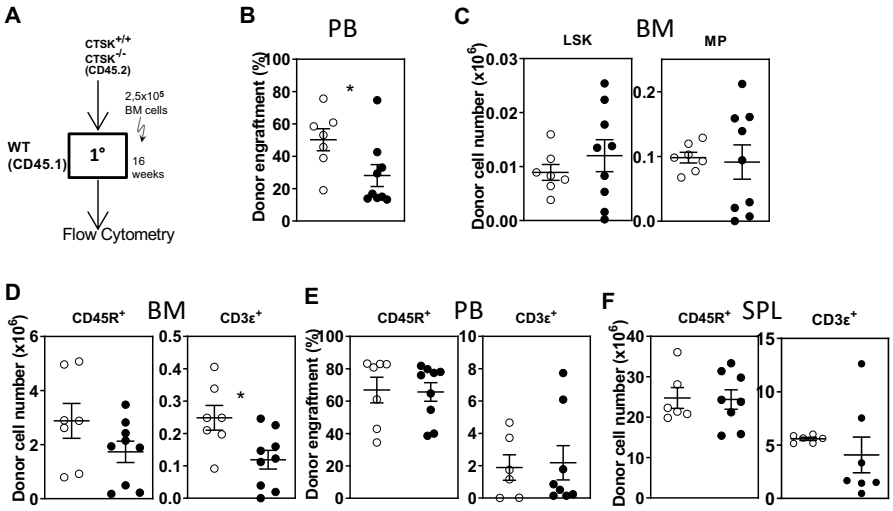

Figure 7 Repopulation capacity of Ctsk -/- HSCs

A Experimental design. CD45.2 BM cells from *Ctsk*$^{-/-}$ and WT controls were transplanted into CD45.1 WT recipient mice and analyzed 16 weeks post transplantation
B Percentage of donor engraftment in the PB (50.2 ± 6.8% for WT donors compared to 28.1 ± 6.8% for *Ctsk*$^{-/-}$ donor mice, $p < .003$)
C Absolute numbers of MPs and CD34^{-} LSKs in the BM of transplanted mice
D Absolute numbers of B and T lymphocytes in the BM (CD3ε+: 24.9 ± 3.4 × 10^4 for WT compared to 11.9 ± 2.8 × 10^4 for *Ctsk*$^{-/-}$ donor mice, $p < .016$)
E Percentage of B and T lymphocytes in the PB
F absolute numbers of B and T lymphocytes in the SPL
Closed white circles represent WT cells, closed black circles represent Ctsk$^{-/-}$ *cells.*

4.5 Characteristics of CD34- LSKS cultured in single cell cultures in the presence or absence of SFRP1

Much like CTSK, SFRP1 is secreted by various niche components, particularly by mesenchymal cells and osteoblasts. While SFRP1 is well-known for its role in antagonizing canonical *Wnt*, evidence shows it also binds to WNT5a and modulates non-canonical *Wnt* signaling (Bischoff et al., 2015; Pereira et al., 2008). Thus, we investigated how the absence of SFRP1 in vitro impacts HSC fate.

Successful silencing of the *Sfrp1* gene in UG26-1B6 sh*Sfrp1* stromal cells was confirmed via qPCR (mean downregulation from four experiments: 92.40%, as shown in **Fig. 8A).**

Similar to the effects observed in cultures with sh*Ctsk* conditioned medium (CM), clone sizes of HSCs cultured in *Sfrp1*-deficient CM were significantly smaller than the control ($p<0.01$ for days 3 and 4, and $p<0.001$ for days 5 and 6, **Fig. 8B**). We also noted a trend towards reduced cell cycle recruitment (time to first division: 51.21±2.41 hours vs. 55.72±1.82 hours for pLKO.1-CM vs. *shSfrp1*-CM, $p=0.19$, **Fig. 8D),** as well as fewer wells with divided cells on days 2 and 3 (**Fig.8E**). Both culture media had similar percentages of wells with detectable cells during the culture period (ranging between 76.2-83% for pLKO.1-CM and 77.6-79% for *shSfrp1*-CM, as shown in **Fig. 8F**). The viability of LSKs (70.75±2.25% vs. 66±1% Annexin V- PI- cells for pLKO.1-CM vs. *shSfrp1*-CM) and MPs (67.8±1.6% vs. 68.9±1.9% Annexin V- PI- cells for pLKO.1-CM vs. *shSfrp1*-CM), as well as the incidence of apoptosis (LSKs: 11.4±0.7% vs. 12.95±0.95% Annexin V+ PI- and MPs: 9.62±0.38% vs. 8.18±0.58% for *pLKO.1*-CM vs. *shSfrp1*-CM), did not differ between knockdown-CM and controls (**Fig. 8G-H**).

Interestingly, the differentiation analysis showed a reduction in the fraction of $B220^{+}$ lymphocytes from CD34-SLAM cells cultured in *shSfrp1*-CM (22±5.00% vs. 5.99±1.67%, $p<0.01$, **Fig. 8I**).

Thus, the lack of SFRP1 in vitro leads to impaired HSC expansion and function.

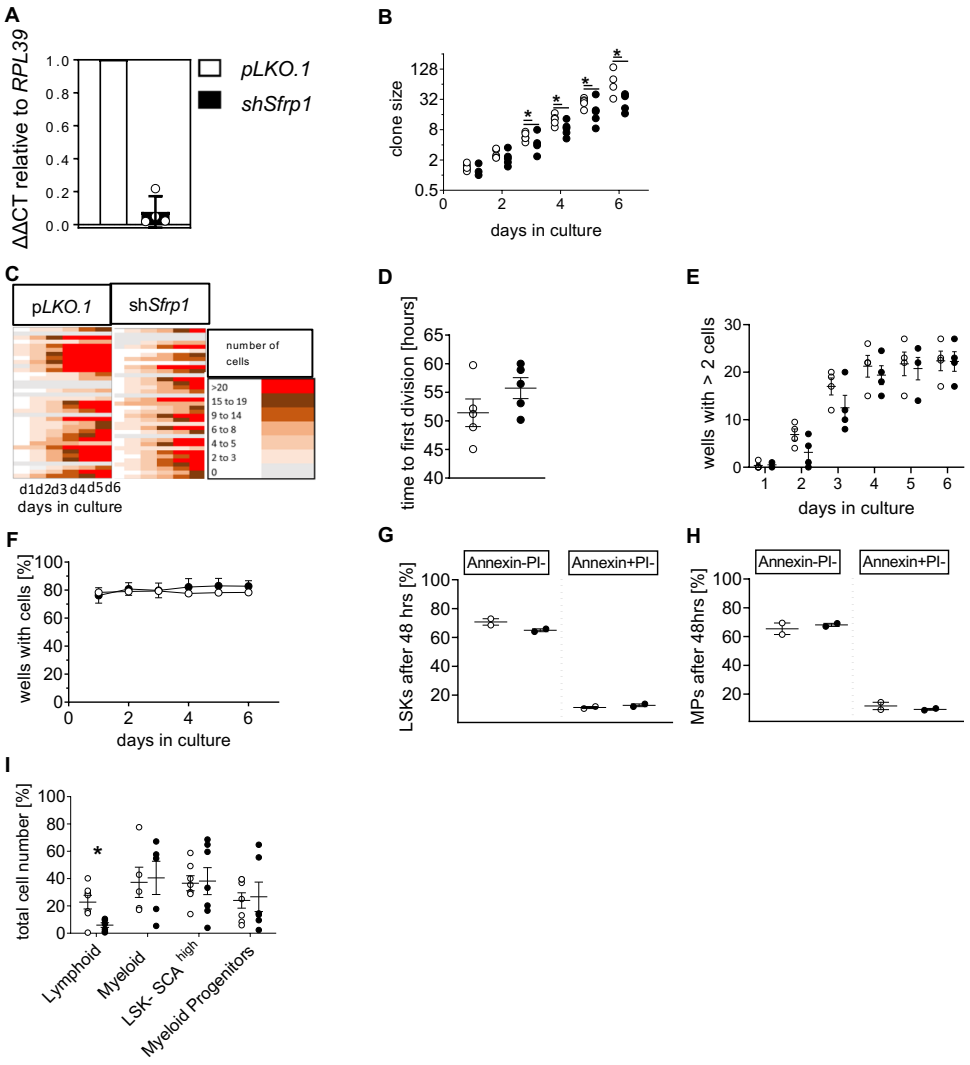

Figure 8 Proliferation, survival, cell division rate, differentiation and of single CD34- SLAM cells on SFRP1 deficient medium

A mRNA content of *Sfrp1* with RPL39 as housekeeping gene in the UG26-1B6 knockdown clone *shSfrp1* and the empty vector control *pLKO.1* measured by realtime-PCR.
B Microscopically evaluated mean clone size of CD34- SLAM cells cultured in *pLKO.1* or *shSfrp1* conditioned medium.
C Heatmap of an exemplary experiment depicting the daily growth of single clones per well colored by number of cell divisions.
D Mean hours elapsed from spotting more than 1 cell in each well.
E Percentage of wells with more than two cells 6 days after culture
F Percentage of wells with detectable cells during each day of culture.
G Percentage of live (Annexin-PI-) and apoptotic (Annexin+PI-) LSKs and **H** MPs
I Percentage of lymphoid and myeloid cells, as well as SCA^{high} and SCA^{low} LSKs and Myeloid Progenitors 6 days after culture of $CD34^{-}$ SLAM cells.
Closed white circles represent cells cultured in pLKO.1-CM, closed black circles represent cells cultured in shSfrp1-CM.

4.6 Identification of small molecule inhibitors and their titration

To identify key nodes within the Sfrp1 and Wnt network influencing HSC behaviour, we performed single-cell cultures supplemented with small molecule inhibitors. Previously, RNA sequencing of wildtype LSKs repopulated in a WNT5A-haploinsufficient niche (Schreck et al., 2017) had revealed a dysregulated expression of genes associated with autophagy, endocytosis, and actin cytoskeleton regulation. An excerpt from the complete data excerpt is provided below (Schreck et al., 2017).

Gene Name	Fold change	p-value (adjusted)	Pathway
Bax	0,42	0,03599	Autophagy pathway
Becn1	0,50	0,04501	Autophagy pathway
Sirt3	0,50	0,02524	Autophagy pathway
Ctsd	0,53	0,00004	Autophagy pathway
Snx14	2,67	0,00080	Autophagy pathway
Ap2b1	0,42	0,00000	Endocytosis
Sh3kbp1	1,42	0,04368	Endocytosis
Arf6	1,59	0,01183	Endocytosis
Inpp5a	0,32	0,00602	Phosphatidylinositol signaling
Inpp5k	0,46	0,00537	Phosphatidylinositol signaling
Ocrl	0,61	0,00920	Phosphatidylinositol signaling
Pik3ip1	1,54	0,02160	Phosphatidylinositol signaling
Plce1	2,48	0,03632	Phosphatidylinositol signaling
Pip5k1a	0,46	0,00294	Regulation of actin cytoskeleton
Dock2	1,58	0,02699	Regulation of actin cytoskeleton
Wasf2	1,94	0,01002	Regulation of actin cytoskeleton
Actn1	2,22	0,03104	Regulation of actin cytoskeleton
Arhgef7	2,27	0,00285	Regulation of actin cytoskeleton
Iqgap3	2,39	0,01090	Regulation of actin cytoskeleton
Scin	2,62	0,02738	Regulation of actin cytoskeleton

Table 16 Excerpt of RNA-Seq results from WT HSC regenerated on WNT5a +/- background. With permission from Prof. RA Oostendorp

A summary of the analyzed inhibitors, their concentrations, and the observed effects is presented in **Table 16**.

Gene	Inhibitor	Concen-tration [µmol]	Effect on HSC proliferation/ differentiation	NO Experiments	Pathway	Fold change
BECN1	Spautin-1	0.03/0.1/0.2/0.6/10	adverse effects	5	Autophagy	0,5
ARF6	SecinH3 #	0.8/2.4/5.4/7.2	pLKO.1-shSfrp1 ↑	6	Endocytosis	1,59
PLCE1	Edelfosine #	1.0/2.5/5.0/10	none	1	Phosphatidyl-inositol signaling	2,48
Pip5k1a	ISA2011B	0.33/1.1/3.3	none	3	Regulation of actin cytoskeleton	0,46
DOCK2	CPYPP	0.91/4.56/7.6/22.8/68	toxic on both CM	2	Regulation of actin cytoskeleton	1,58

Table 17 List of analyzed small molecule inhibitors according to their mechanism of action, tested concentrations, observed effect on HSCs in culture with either pLKO.1 or shSfrp1-CM, number of experiments and pathway.

 # not specific for the gene

4.7 BECN-1 inhibition with Spautin-1 had inconsistent effects on maintenance of CD34- LSKs in single cell cultures

Spautin-1 is an autophagy inhibitor that destabilizes *Becn1* through the deubiquitination and inhibition of enzymes USP10 and USP13 (Liu et al., 2011). *Becn1* is downregulated in wildtype LSKs repopulated in a *Wnt5a*-deficient niche (**Table 15)**. Given that both WNT5a and SFRP1 influence autophagy through interactions with the canonical Wnt pathway, we investigated whether inhibiting autophagy in the presence and absence of SFRP1 yields distinct effects on HSCs.

In single-cell experiments, we added Spautin-1 at varying concentrations to the *pLKO.1*-CM or *shSfrp1*-CM. A concentration of 0.03µM had no impact on survival, proliferation, cell cycle recruitment, or progression (data not shown). When Spautin-1 was administered at 0.1µM, on day 2, cell cycle progression was significantly accelerated in both culture media. Percentages of wells with divided cells increased from 20.67±3.0% for pLKO.1-CM to 57.33±7.22% for pLKO.1+Spautin 0.1µM -CM ($p<0.05$) and 10.34±3.40% vs. 55.34% for sh*Sfrp1*-CM vs. sh*Sfrp1*+ Spautin 0.1µM -CM ($p<0.01$) on day 2 (**Fig.9C**). At Spautin-1

concentrations of 0.2 and 0.6µM, the effects on HSC proliferation and cell cycle in sh*Sfrp1*-CM became inconsistent, while unchanged in HSCs cultured in pLKO.1-CM (**Fig.9A**). This inconsistency could be due to distinct effects of Spautin-1 on different HSC subsets in a SFRP1-deficient environment. Spautin-1 concentrations of 10µM severely impaired proliferation, cell cycle entry, and progression of HSCs in both CM environments, whithout impact on survival (**Fig.9D**), probably due to potential toxicity at this concentration.

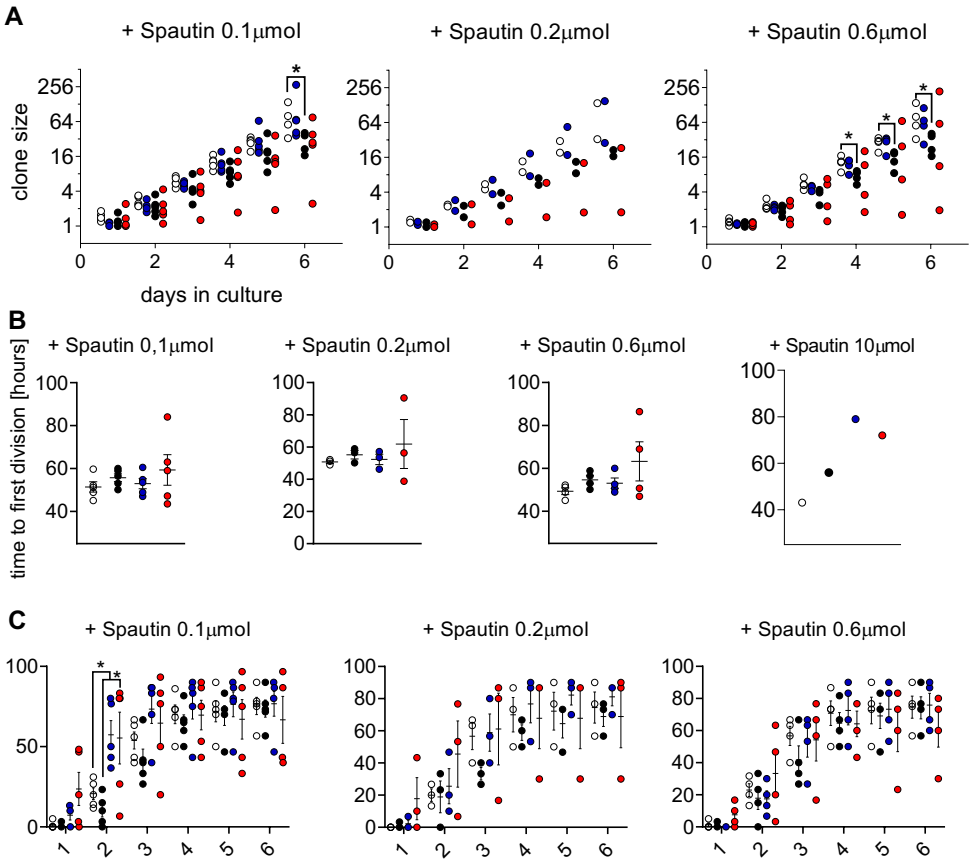

Figure 9 Proliferation, cell cycle recruitment, division, survival and differentiation of single CD34- SLAM cells on Spautin-1 supplemented SFRP1 sufficient and deficient medium

D Percentage of wells containing at least one cell
E Percentage of lymphoid and myeloid cells, as well as SCA^{high} LSKs and Myeloid Progenitors 6 days after culture of CD34^{-} SLAM cells.
Closed white circles represent cells cultured in pLKO.1-CM, closed black circles represent cells cultured in shSfrp1-CM. Closed blue circles represent cells cultured in pLKO.1-CM supplemented with Spautin-1, closed red circles represent cells cultured in shSfrp1-CM supplemented with Spautin-1.

Regarding differentiation, we observed significantly fewer myeloid cells at Spautin-1 concentrations of 0.6µM to the *pLKO.1*-CM (5.17±1.37% vs. 0.17±7.44%, p<0.05, **Fig. 9E**).

In summary, the experiments with Spautin-1 yielded inconsistent effects on HSCs cultured in sh*Sfrp1*-CM at concentrations of 0.1-0.6µM, with the only stable observation being a reduction in myeloid cells cultured in both CM at a concentration of 0.6µM. We discontinued our investigation into Spautin-1 due to the lack of robustly reproducable effects. The number of experiments conducted

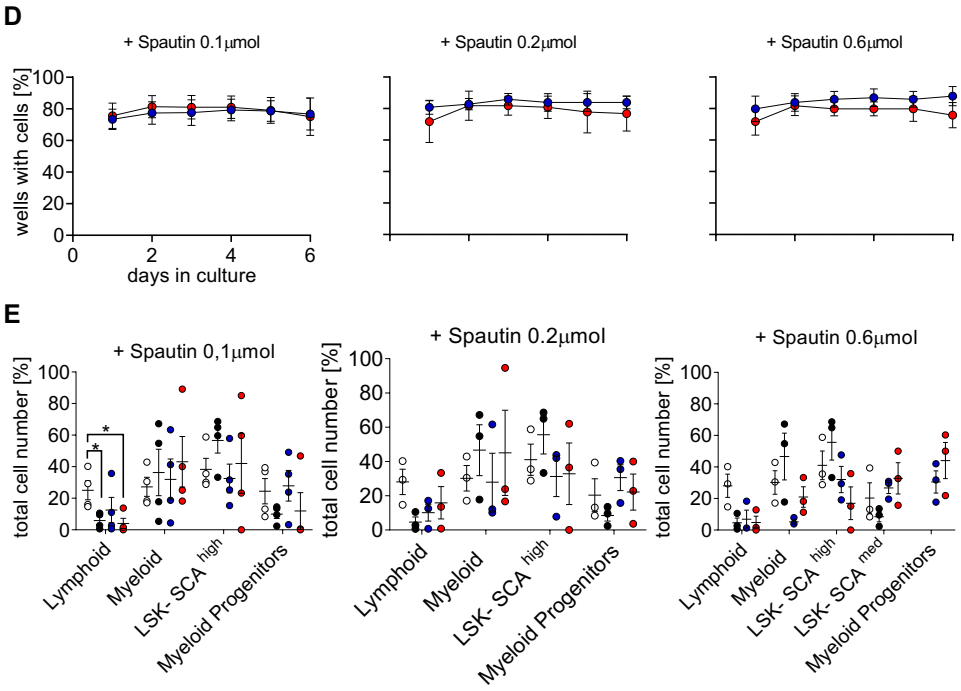

Figure 9 Proliferation, cell cycle recruitment, division, survival and differentiation of single CD34- SLAM cells on Spautin-1 supplemented SFRP1 sufficient and deficient medium

A Microscopically evaluated mean clone size of CD34$^-$ SLAM cells cultured in *pLKO.1* or *shSfrp1* conditioned medium (left) with different concentrations of Spautin-1.
B Mean hours elapsed from spotting more than 1 cell in each well
C Percentage of wells with two or more cells up to 6 days after culture
Closed white circles represent cells cultured in pLKO.1-CM, closed black circles represent cells cultured in shSfrp1-CM. Closed blue circles represent cells cultured in pLKO.1-CM supplemented with Spautin-1, closed red circles represent cells cultured in shSfrp1-CM supplemented with Spautin-1.

for the individual concentrations was limited; the experimental design however was intended as a screening method and was, therefore, feasible.

4.8 Arf6 Inhibition with SecinH3 enhanced proliferation of CD34- LSKs in the absence of Sfrp1

Arf6 is a small GTPase that facilitates the internalization of cell surface receptors and membrane components. It was upregulated by a 1.59-fold in WT LSKs in a Wnt5a-haploinsufficient niche (**Table 15**).

A direct signaling pathway between *Wnt5a* and *Arf6* has not yet been explored. But it's worth noting that both play a crucial role in regulating membrane dynamics and vesicular trafficking. Furthermore, both regulate cell motility and migration. Although at the beginning of this thesis it was unknown, transplantation experiments of early hematopoietic stem cells with a *Cytohesin* 1 knockdown led to severe impairment of long-term engraftment through defects in homing and cell motility (Rak et al., 2017).

SecinH3 is a small molecule inhibitor that selectively targets the small GTPase ARF6 by inhibiting its guanine exchange factors (GEFs), CYTOHESIN1 (CYTH1) and CYTOHESIN2 (CYTH2). The reported IC50 values are 2.4 μM for CYTH1 and 5.6μM for CYTH2, (Hafner et al., 2006).

We examined the effect of SecinH3 at three concentrations: 0.8μM, 2.4μM, and 7.2μM. In all concentrations, SecinH3 rescued the reduced proliferation of HSCs in the sh*Sfrp1*-CM and at concentrations of 2.4μM and 7.2μM, proliferation of HSCs in *shSfrp1*-SecinH3-CM significantly increased compared to HSCs in *pLKO.1*-CM (**Fig. 10A**). The increase in proliferation was probably caused by faster cell cycle progression on days 2 and 3 (mean percentage of wells with divided cells on day 3: 33.88±4.34% for sh*Sfrp1*-CM vs. 54.44±4.44% for sh*Sfrp1*+SecinH3 2.4μM-CM, $p<0.05$, **Fig. 10C**).

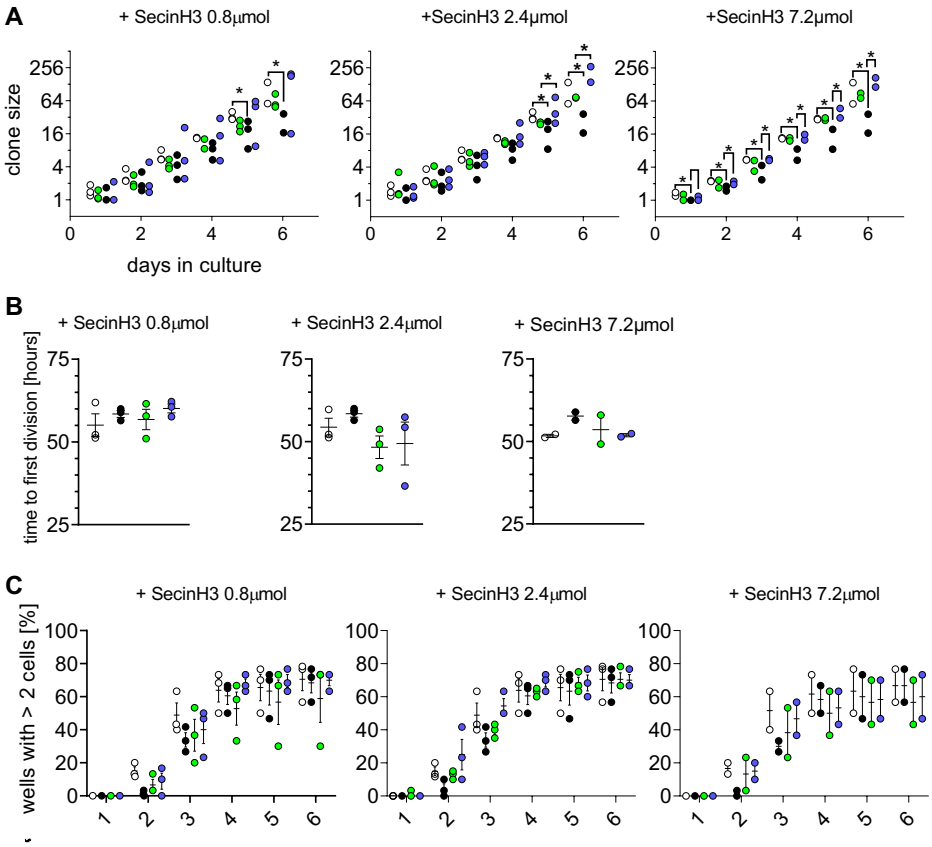

Figure 10 Proliferation, cell cycle recruitment, division, survival and differentiation of single CD34- SLAM cells on SecinH3 supplemented medium in SFRP1 sufficient and deficient environment

A Microscopically evaluated mean clone size of CD34$^-$ SLAM cells cultured in *pLKO.1* or *shSfrp1* conditioned medium (left) with different concentrations of SecinH3**.**
B Mean hours elapsed from spotting more than 1 cell in each well
C Percentage of wells with two or more cells up to 6 days after culture
Closed white circles represent cells cultured in pLKO.1-CM, closed black circles represent cells cultured in shSfrp1-CM. Closed green circles represent cells cultured in pLKO.1-CM supplemented with SecinH3, closed lilac circles represent cells cultured in shSfrp1-CM supplemented with SecinH3.

Interestingly, SecinH3 had no effect on HSCs in *pLKO.1*-CM on any day (mean percentage of wells with divided cells on day 3: 48.89±7.29% for *pLKO.1*-CM vs. 39.45±2.42% for *pLKO.1*+SecinH3 2.4µM-CM). Whilst a similar trend was observed with 7.2µM, the limited number of experiments prevented statistical confirmation of this finding.

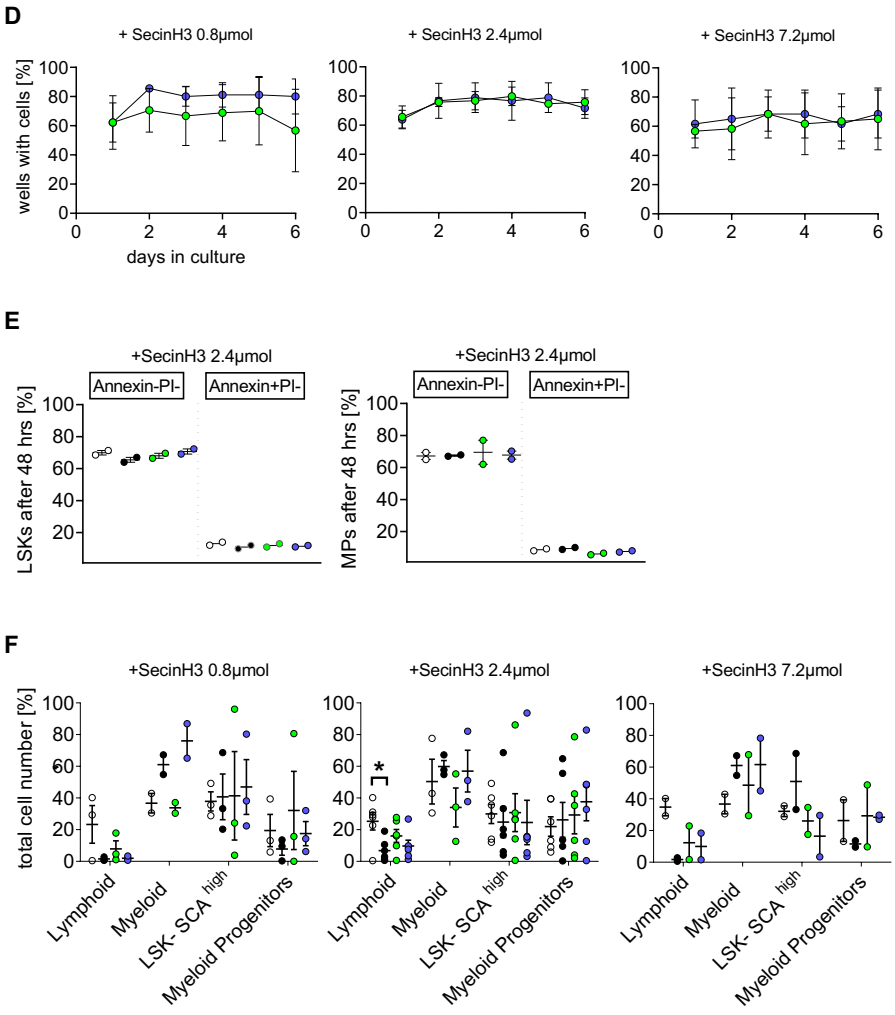

Figure 10 Proliferation, cell cycle recruitment, division, survival and differentiation of single CD34- SLAM cells on SecinH3 supplemented medium in SFRP1 sufficient and deficient environment

D Microscopically evaluated mean clone size of CD34- SLAM cells cultured in *pLKO.1* or *shSfrp1* conditioned medium.
E Percentage of lymphoid and myeloid cells, as well as SCA^{high} LSKs and Myeloid Progenitors 6 days after culture of $CD34^-$ SLAM cells.
F Percentage of live ($Annexin^-PI^-$) and apoptotic ($Annexin^+PI^-$) LSKs and MPs after 2 days culture with 2.4µmol SecinH3
Closed white circles represent cells cultured in pLKO.1-CM, closed black circles represent cells cultured in shSfrp1-CM. Closed green circles represent cells cultured in pLKO.1-CM supplemented with SecinH3, closed lilac circles represent cells cultured in shSfrp1-CM supplemented with SecinH3

SecinH3 also had no impact on cell survival, apoptosis (only tested for concentrations of 2.4µmol), or differentiation (**Fig. 10D-F**).

To summarize, SecinH3 stimulated HSC proliferation in a SFRP1-deficient environment. Partly, proliferation exceeded the observed proliferation rate in the SFRP1-intact control. SecinH3 had no effect on proliferation, cell cycle entry and progression, survival, or differentiation in HSCs cultured in the control-CM. This suggests that the absence of SFRP1 during Arf6 inhibition likely contributed to this phenotype.

4.9 Other tested inhibitors

We tested other small molecule inhibitors.

4.9.1 DOCK2 inhibition with CPYPP

Dedicator of cytokinesis 2 is expressed both in early hematopoietic stem cells and in lymphopoiesis. DOCK is a GEF that activates Rac-GTPases and is involved in regulation of the actin cytoskeleton, mainly in cell adhesion and migration. Steady state hematopoiesis is normal in *Dock2*$^{-/-}$ mice, and also HSC engraftment and self-renewal have been shown to be unimpaired in serial transplantation experiments (Kikuchi et al., 2008). CPYPP (6-chloro-N-(2,3-dihydrobenzo[b][1,4]dioxin-6-yl)-3-pyridinamin) is a small molecule inhibitor that selectively binds to DOCK2 and inhibits Rac-activiation. The previously described IC50 of the CPYPP is 22.8 µmol. In in-vitro assays, it inhibited migration and homing of lymphocytes (Nishikimi et al., 2012).

However, CPYPP did not show any effect on proliferation, survival or differentiation on HSC fate in the smallest concentration of 0.91 µmol in neither pLKO.1 nor shSfrp1 medium, whilst highly impairing proliferation and survival of HSCs in both CM from concentrations of 4.56 µmol or higher, most likely due to toxicity (see **Table 16,** data not shown).

4.9.2 Pip5K1a Inhibition with ISA2011B

Phosphatidylinositol-4-phosphate 5-kinase type 1 alpha is an enzyme that catalyzes the phosphorylation of Phosphatidylinositol 4 phosphate (PIP4) to

phosphatidylinositol 4,5 biphosphate (PIP2). PIP2 regulates the actin cytoskeleton as well as endocytosis and membrane trafficking. It also plays a role in PI3K/AKT signaling, which regulates proliferation and survival.

PIP5K1A has not yet been investigated in primitive hematopoietic stem cells. ISA2011B was developed as a selective Inhibitor for PIP5K1A a in prostate cancer research. Here, overexpression of PIP5K1A was found to be associated with a worse prognosis. ISA2011B induced apoptosis and reduced invasion (Semenas et al., 2014).

Furthermore, inhibitory effects of the small molecule inhibitor ISA2011B on T-cell functions have also been described (Kunkl et al., 2017). ISA2011B did not affect proliferation, differentiation or survival in $CD34^-$ SLAM cells. This could, however, be due to the relatively low concentration of ISA2011B used in the single cell assays compared to concentrations of 10 µmol that had been used in the in vitro assays previously described.

4.9.3 PLCE1 inhibition with Edelfosine

Phospholipase C epsilon 1 is an enzyme of the Phospholipase C family. It catalyzes the hydrolyzation of phospholipids in the cell membrane, mainly PIP2 into inositol 1,4,5-trisphosphate (IP3) and diacylglycerol (DAG). IP3 and DAG are second messengers and required in various cellular processes like metabolism, cell survival and proliferation. PLCE1 is overexpressed in many solid cancers like esophageal squamous cell carcinoma, hepatocellular carcinoma and colorectal carcinoma (Chen et al., 2021; Wang et al., 2020). In regard to hematopoiesis, PLCE1 is an effector of Ras and leads to activation of CD4+ T-cells (Czyzyk et al., 2003), while its role in hematopoietic stem cells has not been investigated. Edelfosine (ET-18-OCH_3) is a PLC inhibitor (Lippman & Hong, 1991) and had proapoptotic effects in solid cancers, lymphomas and leukemias (Mollinedo et al., 2010). However, it did not affect proliferation, differentiation or survival in ESLAM cells.

5. Discussion

5.1. Cathepsin K

In the first part of this thesis, we explored the impact of stromal CTSK on hematopoiesis in vitro and compared it with reanalyzed data from in vivo experiments.

We show that CTSK regulates proliferation of long-term HSCs cultured in stromal conditioned medium in vitro. *Ctsk* knockdown in stromal cells impairs their ability to maintain proliferation and function of early hematopoietic cells. This results in smaller populations with a tendency to myeloid skewing. Lymphopoiesis was not impaired in terms of B-cell numbers. From our experience with the single cell assay, maintenance and proliferation of T- lymphocytes in this assay is generally limited, thus, in vitro, the effect of CTSK could not be accounted for.

CTSK is a protease that cleaves collagen and stem cell factor, two secreted factors that play an essential role in the maintenance of early hematopoietic stem cells in culture conditions (Kollet et al., 2006; Wohrer et al., 2014). Through cleavage of these, it seems plausible for CTSK to modulate HSC behavior. Also, CXCL12 and Osteopontin are known substrates for CTSK (Kollet et al., 2006). Therefore, a secretome analysis could provide valuable insights into the relevant CTSK substrates necessary for the maintenance of hematopoiesis in vitro.

In contrast to our in vitro findings, in vivo, the loss of CTSK was dispensable for early hematopoiesis or myelopoiesis. Interestingly, alterations of lymphopoiesis in various hematopoietic compartments were observed. Our findings are in accordance with data that show that Osteolineage cells maintain lymphopoiesis as CTSK is secreted by osteoclasts.

Our results demonstrate, that cell-extrinsic CTSK regulates both, B- and T-cell repopulation, particularly in the bone marrow and less pronounced in other lymphatic compartments. Our findings match previous experiments by Jardon-Alvarez from our group, who found a reduction of donor bone marrow $CD3\varepsilon^{+}$- T-

lymphocytes and LSKs after transplantation of Lin^- cells that had been co-cultured on UG261B6- sh*Ctsk* stroma into wildtype recipients (Jardon-Alvarez, 2016). These results confirm an impairment of early hematopoietic function observed in vitro. Whilst CTSK seems to be redundant for HSC maintenance in vivo, there is no compensation for the reduced fraction of $CD3\varepsilon^+$- T- lymphocytes.

The loss of cell-intrinsic CTSK nearly exceptionally affects the small $CD3\varepsilon^+$ T-lymphocytic bone marrow compartment. This finding is consistent among 4 different experimental settings and most importantly, apparent in steady – state and transplantation conditions that mimic hematopoietic stress. While the role of the $CD3\varepsilon^+$ T-lymphocyte compartment in the bone marrow has not completely been understood, a small subset of $FoxP3^+$ T- regulatory cells has been implicated in maintaining HSC quiescence in the bone marrow niche (Hirata et al., 2018). Interestingly, $FoxP3^+$ T- regulatory cells deficient in CTSK have been demonstrated to be more potent in suppressing T effector cells (Zhou et al., 2017).

The reduced peripheral engraftment observed in the intrinsic transplantation experiments is most likely due to the reduced absolute number of B- cells across all examined hematopoietic tissues (Hausinger et al., 2021).

The contrast between the necessity of CTSK in vitro and its abundance in vivo may be explained as follows: In UG261B6 cells, CTSK was – among other Cathepsins – the only Cathepsin overexpressed compared to HSC-non-supporting cell lines (Buckley et al., 2011; Oostendorp et al., 2005). Firstly, this unique expression profile is likely to account for the observations in vitro. Secondly, in vivo, *Ctsk* expression is highest in osteoclasts followed by mesenchymal bone marrow niche cells and endothelial cells as well as to a lesser extent in myeloid cells. These cells could compensate for the absent CTSK in stromal cells, a context, that our single cell model and the co-cultures do not depict. Furthermore, there might be a redundancy in HSC regulation by the other Cathepsins Z and S (Bararia et al., 2020; Dera et al., 2019; Rauner et al., 2014). Cathepsin Z is predominantly expressed and secreted by myeloid cells and Cathepsin S by antigen presenting cells. Due to their high structural similarity to

CTSK (Vizovisek et al., 2019), they might compensate for the loss of CTSK in vivo: Staudt et al. for example found that CTSZ secreted by human osteoblasts and stromal cells is able to cleave CXCL12, and reduces cellular adhesion between early HSC and osteoblasts in culture (Staudt et al., 2010), whilst also CTSB and CTSL were able to cleave CXCL12 (Perisic Nanut et al., 2021; Staudt et al., 2012). Research on CTSK focuses on metastatic bone disease (Jiang et al., 2021; Song et al., 2023) and osteoporosis. Research on the impact of CTSK on hematopoietic processes remains scarce (Perisic Nanut et al., 2021). However, our data and those from others investigating CTSK in autoimmunity (Asagiri et al., 2008) indicate immune-regulatory functions. Within the context of the hematopoietic niche, further examination of CTSK and other cathepsins in pathologies like myeloproliferative disorders that display defects in the communication between the hematopoietic niche and HSCs might be interesting.

5.2. Secreted frizzled- related protein 1

The second research question concerned SFRP1 and its potential interaction with the WNT pathway. Previous RNA sequencing of wildtype LSKs repopulated in a *Wnt5a*$^{-/+}$ niche had revealed dysfunctional expression of genes involved in various molecular pathways. For some of them, existing small molecule inhibitors were found and examined for potential impact on the fate of early HSCs.

In single cell experiments with CD34^{-} SLAM cells cultured on *Sfrp1*- knockdown stroma reduced clone size and diminished cell cycle recruitment were observed. Additionally, the number of B220^{+} cells was consistently reduced in the absence of SFRP1, while early hematopoiesis showed a trend towards myeloid skewing. Malhotra et al. demonstrated that the presence of extrinsic WNT3A in co-culture experiments with primitive HSCs suppresses B-lymphopoiesis in vitro, whilst extrinsic WNT5A augments B-lymphopoiesis (Malhotra et al., 2008). In accordance with these findings, single cell cultures with sh*Sfrp1*- conditioned medium exhibit the canonical WNT phenotype. It would have been informative to conduct immunofluorescence analysis of the LSK and stain for ß-Catenin and

WNT3a to confirm increased canonical WNT and for WNT5a and Actin to evaluate for potential inhibition.

In recent experiments, Hettler et al. demonstrated that single-cell cultures with LT-HSCs from $OS1^{\Delta/\Delta}$ mice failing to express SFRP1 specifically in osteoblasts, similarly show decreased clone sizes. Furthermore, proportions of LSK and MP cells were diminished. In immunofluorescence staining, enhanced β-catenin/p300 signaling was found in LT-HSCs (Hettler et al., 2023).

Based on the results of a gene expression analysis of LSKs regenerated in a WNT5A-haploinsufficient niche, we identified several small molecule inhibitors and screened them for effects on LSKs in both SFRP1-knockdown and control conditioned media. An MTT assay was not performed due to the large number of LSKs required for a successful test. Instead, concentrations around the published IC50 values were used in the single-cell assay.

We investigated several small molecule inhibitors.

Spautin-1, a BECN1 inhibitor of autophagy, had inconsistent effects on CD34- SLAM cells cultured in both SFRP1-knockdown and control media. Although cell cycle progression was accelerated on days 2 and 3 after culture in both media, the proliferation of CD34- SLAM cells in SFRP1-knockdown conditioned medium either increased or decreased with Spautin-1. Additionally, Spautin-1 significantly reduced differentiation into myeloid progenitors in both media. No selective effects on LSKs in either conditioned medium were observed. Due to inconsistencies in multiple experiments with concentrations ranging from 0.03 μM to 10 μM, we conclude that Spautin-1 does not have consistent selective effects on early hematopoietic stem cells in either conditioned medium.

Next, we investigated the effects of ARF6 inhibition on $CD34^-$ SLAM cells. ARF6 regulates actin cytoskeleton remodeling (Singh et al., 2020), adhesion and endocytosis. It is activated by its guanine nucleotide exchange factors (GEFs) CYTH1 and CYTH2. Although the role of ARF6 in early hematopoiesis has not

been studied in depth, knockdown of CYTH1 in early HSCs impaired long-term engraftment severely due to defects in homing and cell motility (Rak et al., 2017). Additionally, ARF6 regulates cytoskeletal rearrangement in platelets and neutrophil polarization (Choi et al., 2006; Ren et al., 2020).

The cytohesin-inhibitor SecinH3 selectively stimulated the proliferation of $CD34^-$ SLAM cells by rescuing cell cycle entry in $CD34^-$ SLAM cells in shSfrp1-CM, while having no effect on cells in pLKO.1-CM. Therefore, significantly larger cell clones from day 3 on at concentrations between 2.4 and 7.2 µM were apparent. SecinH3 did not affect differentiation of early HSCs. These results were consistent across multiple experiments, suggesting that inhibition of ARF6 rescues the proliferation of early hematopoietic stem cells in an SFRP1-deficient microenvironment.

This finding is noteworthy because the impairment in hematopoiesis observed in the absence of ARF6 or CYTH1 has been attributed to defects in adhesion and migration. Our results show that ARF6 also plays a role in the proliferation of early hematopoietic stem cells. Further literature research revealed new evidence indicating that in Drosophila wing development, ARF6 is involved upstream in canonical WNT-signaling by redistributing junctional β-Catenin to the cytoplasm but also downstream of the canonical WNT pathway (Marcetteau et al., 2021). ARF6 may regulate canonical WNT signaling by modulating Pangolin - the Drosophila homolog of TCF1, which is a transcription factor in mice that induces the expression of WNT target genes when bound to β-Catenin.

Considering our findings, ARF6 inhibition may potentially inhibit canonical WNT signaling, that is upregulated in culture of LT-HSC on shSfrp1-CM.

To conclude, we identify ARF6 as a potential player in the WNT pathway in early hematopoietic stem cells. Investigating canonical and non-canonical WNT components by immunofluorescence would have been valuable to verify our results. However, the time-consuming and costly nature of screening multiple small molecule inhibitors precluded this. Also, migration and adhesion assays

would have been interesting. Given the new evidence supporting our findings, further investigation into the effects of ARF6 on early hematopoiesis is warranted.

Epigenetic silencing of *Sfrp1* and overactivation of *WNT/ß-Catenin* signaling plays an important role in hematologic diseases like acute myeloid leukemia (AML), in acute lymphoblastic leukemia (ALL) and chronic lymphocytic leukemia (CLL). Especially in AML, suppression of Sfrp1 and other WNT inhibitors (Elyamany et al., 2023) is evident and associated with a worse prognosis. Several WNT-inhibitors have been developed and tested in hematologic and solid malignancies; however, their limiting factor remains high therapy-associated toxicity, often expanding from nausea, fatigue and headache to hemorrhage, bone marrow toxicity and fractures (de Pellegars-Malhortie et al., 2024). Therefore, no WNT-inhibitor has been clinically approved to date. As WNT-signaling is involved in homeostasis of various healthy tissues, selective suppression of WNT-signaling in malignant cells is a major challenge. Further characterization of potential WNT players and their related drugs is necessary.

6. Summary

We demonstrate, that CTSK is required for optimal HSC maintenance and differentiation in vitro. In vivo, autonomous and non- autonomous CTSK is abundant for hematopoiesis, but indispensable for the maintenance of bone marrow T- lymphocytes in steady-state hematopoiesis and under hematopoietic stress.

Further, absence of SFRP1 in vitro induces a canonical WNT-like phenotype in $CD34^-$ SLAM cells with impaired cell cycle recruitment, fewer $B220^+$ cells and a trend toward myeloid skewing.

ARF6 inhibition with the small molecule inhibitor SecinH3 enhances $CD34^-$ SLAM cell proliferation in *Sfrp1*-knockdown cultures compared to controls. This may be caused by ARF6 involvement in canonical WNT signaling in early hematopoietic stem cells.

7. List of Figures

8. List of Tables

9. Acknowledgements

First, I would like to thank Prof. Dr. Robert Oostendorp, who not only offered me the opportunity of this interesting and challenging project, but also supported me with valuable advice and guidance throughout.

I would like to express my sincere thanks to the entire Oostendorp and Götze research groups for the pleasant working environment. I am especially grateful for the advice I received from Dr. Franziska Hettler.

For her technical support during cell sorting, I thank Lynette Henkel from the Department of Microbiology.

My heartfelt thanks go to Dr. Sandra Romero Marquez, who, besides mentoring me throughout the years, became a close friend.

10.Publications

Parts of this work have been published in the following peer-reviewed articles:

1. *__Hausinger R__, *Hackl M, *Jardon Alvarez A, Kehr M, Romero Marquez S, Hettler F, Kehr C, Grziwok S, Schreck C, Peschel C, Istvánffy R, Oostendorp RAJ. Cathepsin K maintains the compartment of bone marrow T lymphocytes in vivo. Immun Inflamm Dis. 2021 Jun;9(2):521-532. doi: 10.1002/iid3.412. Epub 2021 Feb 16. PMID: 33592138; PMCID: PMC8127559.

   * equally contributing first authors

2. Romero Marquez S, Hettler F, **Hausinger R**, Schreck C, Landspersky T, Henkel L, Angerpointner C, Demir IE, Schiemann M, Bassermann F, Götze KS, Istvánffy R, Oostendorp RAJ. Secreted factors from mouse embryonic fibroblasts maintain repopulating function of single cultured hematopoietic stem cells Haematologica. 2021 Oct 1;106(10):2633-2640. doi: 10.3324/haematol.2020.249102. PMID: 33543864

3. Hettler F, Schreck C, Marquez SR, Engleitner T, Vilne B, Landspersky T, Weidner H, **Hausinger R**, Mishra R, Oellinger R, Rauner M, Naumann R, Peschel C, Bassermann F, Rad R, Istvanffy R, Oostendorp RAJ. Osteoprogenitor SFRP1 prevents exhaustion of hematopoietic stem cells via PP2A-PR72/130-mediated regulation of p300. Haematologica. 2023 Feb 1;108(2):490-501. doi: 10.3324/haematol.2022.280760. PMID: 35950533; PMCID: PMC9890018.

11. References

Acebron, S. P., & Niehrs, C. (2016). beta-Catenin-Independent Roles of Wnt/LRP6 Signaling. *Trends Cell Biol*, *26*(12), 956-967. https://doi.org/10.1016/j.tcb.2016.07.009

Asagiri, M., Hirai, T., Kunigami, T., Kamano, S., Gober, H. J., Okamoto, K., Nishikawa, K., Latz, E., Golenbock, D. T., Aoki, K., Ohya, K., Imai, Y., Morishita, Y., Miyazono, K., Kato, S., Saftig, P., & Takayanagi, H. (2008). Cathepsin K-dependent toll-like receptor 9 signaling revealed in experimental arthritis. *Science*, *319*(5863), 624-627. https://doi.org/10.1126/science.1150110

Baba, Y., Garrett, K. P., & Kincade, P. W. (2005). Constitutively active beta-catenin confers multilineage differentiation potential on lymphoid and myeloid progenitors. *Immunity*, *23*(6), 599-609. https://doi.org/10.1016/j.immuni.2005.10.009

Balazs, A. B., Fabian, A. J., Esmon, C. T., & Mulligan, R. C. (2006). Endothelial protein C receptor (CD201) explicitly identifies hematopoietic stem cells in murine bone marrow. *Blood*, *107*(6), 2317-2321. https://doi.org/10.1182/blood-2005-06-2249

Bararia, D., Hildebrand, J. A., Stolz, S., Haebe, S., Alig, S., Trevisani, C. P., Osorio-Barrios, F., Bartoschek, M. D., Mentz, M., Pastore, A., Gaitzsch, E., Heide, M., Jurinovic, V., Rautter, K., Gunawardana, J., Sabdia, M. B., Szczepanowski, M., Richter, J., Klapper, W.,…Weigert, O. (2020). Cathepsin S Alterations Induce a Tumor-Promoting Immune Microenvironment in Follicular Lymphoma. *Cell Rep*, *31*(5), 107522. https://doi.org/10.1016/j.celrep.2020.107522

Benveniste, P., Frelin, C., Janmohamed, S., Barbara, M., Herrington, R., Hyam, D., & Iscove, N. N. (2010). Intermediate-term hematopoietic stem cells with extended but time-limited reconstitution potential. *Cell Stem Cell*, *6*(1), 48-58. https://doi.org/10.1016/j.stem.2009.11.014

Bischoff, D. S., Zhu, J. H., Makhijani, N. S., & Yamaguchi, D. T. (2015). Induction of CXC chemokines in human mesenchymal stem cells by stimulation with secreted frizzled-related proteins through non-canonical Wnt signaling. *World J Stem Cells*, *7*(11), 1262-1273. https://doi.org/10.4252/wjsc.v7.i11.1262

Buckley, S. M., Ulloa-Montoya, F., Abts, D., Oostendorp, R. A., Dzierzak, E., Ekker, S. C., & Verfaillie, C. M. (2011). Maintenance of HSC by Wnt5a secreting AGM-derived stromal cell line. *Exp Hematol*, *39*(1), 114-123 e111-115. https://doi.org/10.1016/j.exphem.2010.09.010

Carrelha, J., Mazzi, S., Winroth, A., Hagemann-Jensen, M., Ziegenhain, C., Hogstrand, K., Seki, M., Brennan, M. S., Lehander, M., Wu, B., Meng, Y., Markljung, E., Norfo, R., Ishida, H., Belander Stralin, K., Grasso, F., Simoglou Karali, C., Aliouat, A., Hillen, A.,…Jacobsen, S. E. W. (2024). Alternative platelet

differentiation pathways initiated by nonhierarchically related hematopoietic stem cells. *Nat Immunol*, *25*(6), 1007-1019. https://doi.org/10.1038/s41590-024-01845-6

Challen, G. A., Boles, N. C., Chambers, S. M., & Goodell, M. A. (2010). Distinct hematopoietic stem cell subtypes are differentially regulated by TGF-beta1. *Cell Stem Cell*, *6*(3), 265-278. https://doi.org/10.1016/j.stem.2010.02.002

Chen, Z., Chen, H., Yang, L., Li, X., & Wang, Z. (2021). CircPLCE1 facilitates the malignant progression of colorectal cancer by repressing the SRSF2-dependent PLCE1 pre-RNA splicing. *J Cell Mol Med*, *25*(15), 7244-7256. https://doi.org/10.1111/jcmm.16753

Choi, W., Karim, Z. A., & Whiteheart, S. W. (2006). Arf6 plays an early role in platelet activation by collagen and convulxin. *Blood*, *107*(8), 3145-3152. https://doi.org/10.1182/blood-2005-09-3563

Czyzyk, J., Brogdon, J. L., Badou, A., Henegariu, O., Preston Hurlburt, P., Flavell, R., & Bottomly, K. (2003). Activation of CD4 T cells by Raf-independent effectors of Ras. *Proc Natl Acad Sci U S A*, *100*(10), 6003-6008. https://doi.org/10.1073/pnas.1031494100

de Pellegars-Malhortie, A., Picque Lasorsa, L., Mazard, T., Granier, F., & Prevostel, C. (2024). Why Is Wnt/beta-Catenin Not Yet Targeted in Routine Cancer Care? *Pharmaceuticals (Basel)*, *17*(7). https://doi.org/10.3390/ph17070949

Deng, J., Tan, Y., Xu, Z., & Wang, H. (2024). Advances in hematopoietic stem cells ex vivo expansion associated with bone marrow niche. *Ann Hematol*. https://doi.org/10.1007/s00277-024-05773-1

Dera, A. A., Ranganath, L., Barraclough, R., Vinjamuri, S., Hamill, S., & Barraclough, D. L. (2019). Cathepsin Z as a novel potential biomarker for osteoporosis. *Sci Rep*, *9*(1), 9752. https://doi.org/10.1038/s41598-019-46068-0

Ding, L., Saunders, T. L., Enikolopov, G., & Morrison, S. J. (2012). Endothelial and perivascular cells maintain haematopoietic stem cells. *Nature*, *481*(7382), 457-462. https://doi.org/10.1038/nature10783

Dufourcq, P., Descamps, B., Tojais, N. F., Leroux, L., Oses, P., Daret, D., Moreau, C., Lamaziere, J. M., Couffinhal, T., & Duplaa, C. (2008). Secreted frizzled-related protein-1 enhances mesenchymal stem cell function in angiogenesis and contributes to neovessel maturation. *Stem Cells*, *26*(11), 2991-3001. https://doi.org/10.1634/stemcells.2008-0372

Dykstra, B., Kent, D., Bowie, M., McCaffrey, L., Hamilton, M., Lyons, K., Lee, S. J., Brinkman, R., & Eaves, C. (2007). Long-term propagation of distinct hematopoietic differentiation programs in vivo. *Cell Stem Cell*, *1*(2), 218-229. https://doi.org/10.1016/j.stem.2007.05.015

Elyamany, G., Rizwan, H., Akhter, A., Aljabry, M. S., Alotaibi, S., Albalawi, M. A. H., Shabani-Rad, M. T., Roshan, T. M., & Mansoor, A. (2023). "Losing the Brakes"-Suppressed Inhibitors Triggering Uncontrolled Wnt/ss-Catenin Signaling May Provide a Potential Therapeutic Target in Elderly Acute Myeloid Leukemia. *Curr Issues Mol Biol*, *45*(1), 604-613. https://doi.org/10.3390/cimb45010040

Fleming, H. E., Janzen, V., Lo Celso, C., Guo, J., Leahy, K. M., Kronenberg, H. M., & Scadden, D. T. (2008). Wnt signaling in the niche enforces hematopoietic stem cell quiescence and is necessary to preserve self-renewal in vivo. *Cell Stem Cell*, *2*(3), 274-283. https://doi.org/10.1016/j.stem.2008.01.003

Frobel, J., Landspersky, T., Percin, G., Schreck, C., Rahmig, S., Ori, A., Nowak, D., Essers, M., Waskow, C., & Oostendorp, R. A. J. (2021). The Hematopoietic Bone Marrow Niche Ecosystem. *Front Cell Dev Biol*, *9*, 705410. https://doi.org/10.3389/fcell.2021.705410

Greenbaum, A., Hsu, Y. M., Day, R. B., Schuettpelz, L. G., Christopher, M. J., Borgerding, J. N., Nagasawa, T., & Link, D. C. (2013). CXCL12 in early mesenchymal progenitors is required for haematopoietic stem-cell maintenance. *Nature*, *495*(7440), 227-230. https://doi.org/10.1038/nature11926

Hackl, M. (2016). *The Role of Cathepsin K in Hematopoiesis* Technical University of Munich]. Mediatum. https://nbn-resolving.de/urn/resolver.pl?urn:nbn:de:bvb:91-diss-20160118-1243352-1-1

Hafner, M., Schmitz, A., Grune, I., Srivatsan, S. G., Paul, B., Kolanus, W., Quast, T., Kremmer, E., Bauer, I., & Famulok, M. (2006). Inhibition of cytohesins by SecinH3 leads to hepatic insulin resistance. *Nature*, *444*(7121), 941-944. https://doi.org/10.1038/nature05415

Hausinger, R., Hackl, M., Jardon Alvarez, A., Kehr, M., Romero Marquez, S., Hettler, F., Kehr, C., Grziwok, S., Schreck, C., Peschel, C., Istvanffy, R., & Oostendorp, R. A. J. (2021). Cathepsin K maintains the compartment of bone marrow T lymphocytes in vivo. *Immun Inflamm Dis*, *9*(2), 521-532. https://doi.org/10.1002/iid3.412

He, T. C., Sparks, A. B., Rago, C., Hermeking, H., Zawel, L., da Costa, L. T., Morin, P. J., Vogelstein, B., & Kinzler, K. W. (1998). Identification of c-MYC as a target of the APC pathway. *Science*, *281*(5382), 1509-1512. https://doi.org/10.1126/science.281.5382.1509

Hettler, F., Schreck, C., Marquez, S. R., Engleitner, T., Vilne, B., Landspersky, T., Weidner, H., Hausinger, R., Mishra, R., Oellinger, R., Rauner, M., Naumann, R., Peschel, C., Bassermann, F., Rad, R., Istvanffy, R., & Oostendorp, R. A. J. (2023). Osteoprogenitor SFRP1 prevents exhaustion of hematopoietic stem cells via PP2A-PR72/130-mediated regulation of p300. *Haematologica*, *108*(2), 490-501. https://doi.org/10.3324/haematol.2022.280760

Hirata, Y., Furuhashi, K., Ishii, H., Li, H. W., Pinho, S., Ding, L., Robson, S. C., Frenette, P. S., & Fujisaki, J. (2018). CD150(high) Bone Marrow Tregs Maintain Hematopoietic Stem Cell Quiescence and Immune Privilege via Adenosine. *Cell Stem Cell*, *22*(3), 445-453 e445. https://doi.org/10.1016/j.stem.2018.01.017

Jardon-Alvarez, A. (2016). *The role of Cathepsin K in haematopoiesis* Technical University of Munich]. Mediatum. https://mediatum-ub-tum-de.eaccess.tum.edu/?id=1285276

Jiang, F., Liu, H., Peng, F., Liu, Z., Ding, K., Song, J., Li, L., Chen, J., Shao, Q., Yan, S., De Veirman, K., Vanderkerken, K., & Fu, R. (2021). Complement C3a activates osteoclasts by regulating the PI3K/PDK1/SGK3 pathway in patients with multiple myeloma. *Cancer Biol Med*, *18*(3), 721-733. https://doi.org/10.20892/j.issn.2095-3941.2020.0430

Kehr, M. (2017). *Die Untersuchung von Kathepsin K (Ctsk) negativen Stammzellen in der Hämatopoese* Technical University of Munich]. Mediatum. https://nbn-resolving.de/urn/resolver.pl?urn:nbn:de:bvb:91-diss-20170706-1306572-1-0

Kent, D. G., Dykstra, B. J., & Eaves, C. J. (2016). Isolation and Assessment of Single Long-Term Reconstituting Hematopoietic Stem Cells from Adult Mouse Bone Marrow. *Curr Protoc Stem Cell Biol*, *38*, 2A 4 1-2A 4 24. https://doi.org/10.1002/cpsc.10

Kiel, M. J., He, S., Ashkenazi, R., Gentry, S. N., Teta, M., Kushner, J. A., Jackson, T. L., & Morrison, S. J. (2007). Haematopoietic stem cells do not asymmetrically segregate chromosomes or retain BrdU. *Nature*, *449*(7159), 238-242. https://doi.org/10.1038/nature06115

Kiel, M. J., Yilmaz, O. H., Iwashita, T., Yilmaz, O. H., Terhorst, C., & Morrison, S. J. (2005). SLAM family receptors distinguish hematopoietic stem and progenitor cells and reveal endothelial niches for stem cells. *Cell*, *121*(7), 1109-1121. https://doi.org/10.1016/j.cell.2005.05.026

Kikuchi, T., Kubonishi, S., Shibakura, M., Namba, N., Matsui, T., Fukui, Y., Tanimoto, M., & Katayama, Y. (2008). Dock2 participates in bone marrow lympho-hematopoiesis. *Biochem Biophys Res Commun*, *367*(1), 90-96. https://doi.org/10.1016/j.bbrc.2007.12.093

Kirstetter, P., Anderson, K., Porse, B. T., Jacobsen, S. E., & Nerlov, C. (2006). Activation of the canonical Wnt pathway leads to loss of hematopoietic stem cell repopulation and multilineage differentiation block. *Nat Immunol*, *7*(10), 1048-1056. https://doi.org/10.1038/ni1381

Klein, G., Schmal, O., & Aicher, W. K. (2015). Matrix metalloproteinases in stem cell mobilization. *Matrix Biol*, *44-46*, 175-183. https://doi.org/10.1016/j.matbio.2015.01.011

Kollet, O., Dar, A., Shivtiel, S., Kalinkovich, A., Lapid, K., Sztainberg, Y., Tesio, M., Samstein, R. M., Goichberg, P., Spiegel, A., Elson, A., & Lapidot, T. (2006). Osteoclasts degrade endosteal components and promote mobilization of hematopoietic progenitor cells. *Nat Med*, *12*(6), 657-664. https://doi.org/10.1038/nm1417

Kunkl, M., Porciello, N., Mastrogiovanni, M., Capuano, C., Lucantoni, F., Moretti, C., Persson, J. L., Galandrini, R., Buzzetti, R., & Tuosto, L. (2017). ISA-2011B, a Phosphatidylinositol 4-Phosphate 5-Kinase alpha Inhibitor, Impairs CD28-Dependent Costimulatory and Pro-inflammatory Signals in Human T Lymphocytes. *Front Immunol*, *8*, 502. https://doi.org/10.3389/fimmu.2017.00502

Laurenti, E., & Gottgens, B. (2018). From haematopoietic stem cells to complex differentiation landscapes. *Nature*, *553*(7689), 418-426. https://doi.org/10.1038/nature25022

Liang, H., Chen, Q., Coles, A. H., Anderson, S. J., Pihan, G., Bradley, A., Gerstein, R., Jurecic, R., & Jones, S. N. (2003). Wnt5a inhibits B cell proliferation and functions as a tumor suppressor in hematopoietic tissue. *Cancer Cell*, *4*(5), 349-360. https://doi.org/10.1016/s1535-6108(03)00268-x

Lippman, S. M., & Hong, W. K. (1991). Beta-carotene didn't prevent cancer: what's up doc? *J Natl Cancer Inst*, *83*(15), 1110-1111. https://doi.org/10.1093/jnci/83.15.1110

Liu, J., Cui, Z., Wang, F., Yao, Y., Yu, G., Liu, J., Cao, D., Niu, S., You, M., Sun, Z., Lian, D., Zhao, T., Kang, Y., Zhao, Y., Xue, H. H., & Yu, S. (2019). Lrp5 and Lrp6 are required for maintaining self-renewal and differentiation of hematopoietic stem cells. *FASEB J*, *33*(4), 5615-5625. https://doi.org/10.1096/fj.201802072R

Liu, J., Xia, H., Kim, M., Xu, L., Li, Y., Zhang, L., Cai, Y., Norberg, H. V., Zhang, T., Furuya, T., Jin, M., Zhu, Z., Wang, H., Yu, J., Li, Y., Hao, Y., Choi, A., Ke, H., Ma, D., & Yuan, J. (2011). Beclin1 controls the levels of p53 by regulating the deubiquitination activity of USP10 and USP13. *Cell*, *147*(1), 223-234. https://doi.org/10.1016/j.cell.2011.08.037

Malhotra, S., Baba, Y., Garrett, K. P., Staal, F. J., Gerstein, R., & Kincade, P. W. (2008). Contrasting responses of lymphoid progenitors to canonical and noncanonical Wnt signals. *J Immunol*, *181*(6), 3955-3964. https://doi.org/10.4049/jimmunol.181.6.3955

Marcetteau, J., Matusek, T., Luton, F., & Therond, P. P. (2021). Arf6 is necessary for senseless expression in response to wingless signalling during Drosophila wing development. *Biol Open*, *10*(12). https://doi.org/10.1242/bio.058892

Matsuyama, M., Aizawa, S., & Shimono, A. (2009). Sfrp controls apicobasal polarity and oriented cell division in developing gut epithelium. *PLoS Genet*, *5*(3), e1000427. https://doi.org/10.1371/journal.pgen.1000427

Mendez-Ferrer, S., Michurina, T. V., Ferraro, F., Mazloom, A. R., Macarthur, B. D., Lira, S. A., Scadden, D. T., Ma'ayan, A., Enikolopov, G. N., & Frenette, P. S. (2010). Mesenchymal and haematopoietic stem cells form a unique bone marrow niche. *Nature*, *466*(7308), 829-834. https://doi.org/10.1038/nature09262

Mollinedo, F., de la Iglesia-Vicente, J., Gajate, C., Estella-Hermoso de Mendoza, A., Villa-Pulgarin, J. A., de Frias, M., Roue, G., Gil, J., Colomer, D., Campanero, M. A., & Blanco-Prieto, M. J. (2010). In vitro and In vivo selective antitumor activity of Edelfosine against mantle cell lymphoma and chronic lymphocytic leukemia involving lipid rafts. *Clin Cancer Res*, *16*(7), 2046-2054. https://doi.org/10.1158/1078-0432.CCR-09-2456

Nakajima, H., Ito, M., Morikawa, Y., Komori, T., Fukuchi, Y., Shibata, F., Okamoto, S., & Kitamura, T. (2009). Wnt modulators, SFRP-1, and SFRP-2 are expressed in osteoblasts and differentially regulate hematopoietic stem cells. *Biochem Biophys Res Commun*, *390*(1), 65-70. https://doi.org/10.1016/j.bbrc.2009.09.067

Nemeth, M. J., Mak, K. K., Yang, Y., & Bodine, D. M. (2009). beta-Catenin expression in the bone marrow microenvironment is required for long-term maintenance of primitive hematopoietic cells. *Stem Cells*, *27*(5), 1109-1119. https://doi.org/10.1002/stem.32

Nemeth, M. J., Topol, L., Anderson, S. M., Yang, Y., & Bodine, D. M. (2007). Wnt5a inhibits canonical Wnt signaling in hematopoietic stem cells and enhances repopulation. *Proc Natl Acad Sci U S A*, *104*(39), 15436-15441. https://doi.org/10.1073/pnas.0704747104

Niehrs, C., & Acebron, S. P. (2012). Mitotic and mitogenic Wnt signalling. *EMBO J*, *31*(12), 2705-2713. https://doi.org/10.1038/emboj.2012.124

Nishikimi, A., Uruno, T., Duan, X., Cao, Q., Okamura, Y., Saitoh, T., Saito, N., Sakaoka, S., Du, Y., Suenaga, A., Kukimoto-Niino, M., Miyano, K., Gotoh, K., Okabe, T., Sanematsu, F., Tanaka, Y., Sumimoto, H., Honma, T., Yokoyama, S.,…Fukui, Y. (2012). Blockade of inflammatory responses by a small-molecule inhibitor of the Rac activator DOCK2. *Chem Biol*, *19*(4), 488-497. https://doi.org/10.1016/j.chembiol.2012.03.008

Nusse, R., & Clevers, H. (2017). Wnt/beta-Catenin Signaling, Disease, and Emerging Therapeutic Modalities. *Cell*, *169*(6), 985-999. https://doi.org/10.1016/j.cell.2017.05.016

Oguro, H., Ding, L., & Morrison, S. J. (2013). SLAM family markers resolve functionally distinct subpopulations of hematopoietic stem cells and multipotent progenitors. *Cell Stem Cell*, *13*(1), 102-116. https://doi.org/10.1016/j.stem.2013.05.014

Omatsu, Y., Sugiyama, T., Kohara, H., Kondoh, G., Fujii, N., Kohno, K., & Nagasawa, T. (2010). The essential functions of adipo-osteogenic progenitors as the hematopoietic stem and progenitor cell niche. *Immunity*, *33*(3), 387-399. https://doi.org/10.1016/j.immuni.2010.08.017

Oostendorp, R. A., Harvey, K. N., Kusadasi, N., de Bruijn, M. F., Saris, C., Ploemacher, R. E., Medvinsky, A. L., & Dzierzak, E. A. (2002). Stromal cell lines from mouse aorta-gonads-mesonephros subregions are potent supporters of hematopoietic stem cell activity. *Blood*, *99*(4), 1183-1189. https://doi.org/10.1182/blood.v99.4.1183

Oostendorp, R. A., Robin, C., Steinhoff, C., Marz, S., Brauer, R., Nuber, U. A., Dzierzak, E. A., & Peschel, C. (2005). Long-term maintenance of hematopoietic stem cells does not require contact with embryo-derived stromal cells in cocultures. *Stem Cells*, *23*(6), 842-851. https://doi.org/10.1634/stemcells.2004-0120

Osawa, M., Hanada, K., Hamada, H., & Nakauchi, H. (1996). Long-term lymphohematopoietic reconstitution by a single CD34-low/negative hematopoietic stem cell. *Science*, *273*(5272), 242-245. https://doi.org/10.1126/science.273.5272.242

Pereira, C., Schaer, D. J., Bachli, E. B., Kurrer, M. O., & Schoedon, G. (2008). Wnt5A/CaMKII signaling contributes to the inflammatory response of macrophages and is a target for the antiinflammatory action of activated protein C and interleukin-10. *Arterioscler Thromb Vasc Biol*, *28*(3), 504-510. https://doi.org/10.1161/ATVBAHA.107.157438

Perisic Nanut, M., Pecar Fonovic, U., Jakos, T., & Kos, J. (2021). The Role of Cysteine Peptidases in Hematopoietic Stem Cell Differentiation and Modulation of Immune System Function. *Front Immunol*, *12*, 680279. https://doi.org/10.3389/fimmu.2021.680279

Pinho, S., & Frenette, P. S. (2019). Haematopoietic stem cell activity and interactions with the niche. *Nat Rev Mol Cell Biol*, *20*(5), 303-320. https://doi.org/10.1038/s41580-019-0103-9

Rak, J., Foster, K., Potrzebowska, K., Talkhoncheh, M. S., Miharada, N., Komorowska, K., Torngren, T., Kvist, A., Borg, A., Svensson, L., Bonnet, D., & Larsson, J. (2017). Cytohesin 1 regulates homing and engraftment of human hematopoietic stem and progenitor cells. *Blood*, *129*(8), 950-958. https://doi.org/10.1182/blood-2016-06-720649

Rauner, M., Foger-Samwald, U., Kurz, M. F., Brunner-Kubath, C., Schamall, D., Kapfenberger, A., Varga, P., Kudlacek, S., Wutzl, A., Hoger, H., Zysset, P. K., Shi, G. P., Hofbauer, L. C., Sipos, W., & Pietschmann, P. (2014). Cathepsin S controls adipocytic and osteoblastic differentiation, bone turnover, and bone microarchitecture. *Bone*, *64*, 281-287. https://doi.org/10.1016/j.bone.2014.04.022

Ren, C., Yuan, Q., Jian, X., Randazzo, P. A., Tang, W., & Wu, D. (2020). Small GTPase ARF6 Is a Coincidence-Detection Code for RPH3A Polarization in Neutrophil Polarization. *J Immunol*, *204*(4), 1012-1021. https://doi.org/10.4049/jimmunol.1901080

Renstrom, J., Istvanffy, R., Gauthier, K., Shimono, A., Mages, J., Jardon-Alvarez, A., Kroger, M., Schiemann, M., Busch, D. H., Esposito, I., Lang, R., Peschel, C., & Oostendorp, R. A. (2009). Secreted frizzled-related protein 1 extrinsically regulates cycling activity and maintenance of hematopoietic stem cells. *Cell Stem Cell*, *5*(2), 157-167. https://doi.org/10.1016/j.stem.2009.05.020

Rodriguez-Fraticelli, A. E., & Camargo, F. (2021). Systems analysis of hematopoiesis using single-cell lineage tracing. *Curr Opin Hematol*, *28*(1), 18-27. https://doi.org/10.1097/MOH.0000000000000624

Rodriguez-Fraticelli, A. E., Wolock, S. L., Weinreb, C. S., Panero, R., Patel, S. H., Jankovic, M., Sun, J., Calogero, R. A., Klein, A. M., & Camargo, F. D. (2018). Clonal analysis of lineage fate in native haematopoiesis. *Nature*, *553*(7687), 212-216. https://doi.org/10.1038/nature25168

Sarabia-Sanchez, M. A., & Robles-Flores, M. (2024). WNT Signaling in Stem Cells: A Look into the Non-Canonical Pathway. *Stem Cell Rev Rep*, *20*(1), 52-66. https://doi.org/10.1007/s12015-023-10610-5

Schaniel, C., Sirabella, D., Qiu, J., Niu, X., Lemischka, I. R., & Moore, K. A. (2011). Wnt-inhibitory factor 1 dysregulation of the bone marrow niche exhausts hematopoietic stem cells. *Blood*, *118*(9), 2420-2429. https://doi.org/10.1182/blood-2010-09-305664

Schneider, J., Arraf, A. A., Grinstein, M., Yelin, R., & Schultheiss, T. M. (2015). Wnt signaling orients the proximal-distal axis of chick kidney nephrons. *Development*, *142*(15), 2686-2695. https://doi.org/10.1242/dev.123968

Schreck, C., Bock, F., Grziwok, S., Oostendorp, R. A., & Istvanffy, R. (2014). Regulation of hematopoiesis by activators and inhibitors of Wnt signaling from the niche. *Ann N Y Acad Sci*, *1310*, 32-43. https://doi.org/10.1111/nyas.12384

Schreck, C., Istvanffy, R., Ziegenhain, C., Sippenauer, T., Ruf, F., Henkel, L., Gartner, F., Vieth, B., Florian, M. C., Mende, N., Taubenberger, A., Prendergast, A., Wagner, A., Pagel, C., Grziwok, S., Gotze, K. S., Guck, J., Dean, D. C., Massberg, S.,…Oostendorp, R. A. (2017). Niche WNT5A regulates the actin cytoskeleton during regeneration of hematopoietic stem cells. *J Exp Med*, *214*(1), 165-181. https://doi.org/10.1084/jem.20151414

Semenas, J., Hedblom, A., Miftakhova, R. R., Sarwar, M., Larsson, R., Shcherbina, L., Johansson, M. E., Harkonen, P., Sterner, O., & Persson, J. L. (2014). The role of PI3K/AKT-related PIP5K1alpha and the discovery of its selective inhibitor for

treatment of advanced prostate cancer. *Proc Natl Acad Sci U S A*, *111*(35), E3689-3698. https://doi.org/10.1073/pnas.1405801111

Singh, V., Davidson, A. C., Hume, P. J., & Koronakis, V. (2020). Arf6 Can Trigger Wave Regulatory Complex-Dependent Actin Assembly Independent of Arno. *Int J Mol Sci*, *21*(7). https://doi.org/10.3390/ijms21072457

Song, Z., Miao, J., Miao, M., Cheng, B., Li, S., Liu, Y., Miao, Q., Li, Q., & Gao, M. (2023). Cathepsin K-Activated Probe for Fluoro-Photoacoustic Imaging of Early Osteolytic Metastasis. *Adv Sci (Weinh)*, *10*(24), e2300217. https://doi.org/10.1002/advs.202300217

Staal, F. J., Luis, T. C., & Tiemessen, M. M. (2008). WNT signalling in the immune system: WNT is spreading its wings. *Nat Rev Immunol*, *8*(8), 581-593. https://doi.org/10.1038/nri2360

Staudt, N. D., Aicher, W. K., Kalbacher, H., Stevanovic, S., Carmona, A. K., Bogyo, M., & Klein, G. (2010). Cathepsin X is secreted by human osteoblasts, digests CXCL-12 and impairs adhesion of hematopoietic stem and progenitor cells to osteoblasts. *Haematologica*, *95*(9), 1452-1460. https://doi.org/10.3324/haematol.2009.018671

Staudt, N. D., Maurer, A., Spring, B., Kalbacher, H., Aicher, W. K., & Klein, G. (2012). Processing of CXCL12 by different osteoblast-secreted cathepsins. *Stem Cells Dev*, *21*(11), 1924-1935. https://doi.org/10.1089/scd.2011.0307

Sugimura, R., He, X. C., Venkatraman, A., Arai, F., Box, A., Semerad, C., Haug, J. S., Peng, L., Zhong, X. B., Suda, T., & Li, L. (2012). Noncanonical Wnt signaling maintains hematopoietic stem cells in the niche. *Cell*, *150*(2), 351-365. https://doi.org/10.1016/j.cell.2012.05.041

Sugiyama, T., Kohara, H., Noda, M., & Nagasawa, T. (2006). Maintenance of the hematopoietic stem cell pool by CXCL12-CXCR4 chemokine signaling in bone marrow stromal cell niches. *Immunity*, *25*(6), 977-988. https://doi.org/10.1016/j.immuni.2006.10.016

Vizovisek, M., Fonovic, M., & Turk, B. (2019). Cysteine cathepsins in extracellular matrix remodeling: Extracellular matrix degradation and beyond. *Matrix Biol*, *75-76*, 141-159. https://doi.org/10.1016/j.matbio.2018.01.024

Wang, X. K., Liao, X. W., Yang, C. K., Liu, Z. Q., Han, Q. F., Zhou, X., Zhang, L. B., Deng, T., Gong, Y. Z., Huang, J. L., Huang, R., Han, C. Y., Yu, T. D., Su, H., Ye, X. P., Peng, T., & Zhu, G. Z. (2020). Oncogene PLCE1 may be a diagnostic biomarker and prognostic biomarker by influencing cell cycle, proliferation, migration, and invasion ability in hepatocellular carcinoma cell lines. *J Cell Physiol*, *235*(10), 7003-7017. https://doi.org/10.1002/jcp.29596

Wei, Q., & Frenette, P. S. (2018). Niches for Hematopoietic Stem Cells and Their Progeny. *Immunity*, *48*(4), 632-648. https://doi.org/10.1016/j.immuni.2018.03.024

Wilson, A., Oser, G. M., Jaworski, M., Blanco-Bose, W. E., Laurenti, E., Adolphe, C., Essers, M. A., Macdonald, H. R., & Trumpp, A. (2007). Dormant and self-renewing hematopoietic stem cells and their niches. *Ann N Y Acad Sci*, *1106*, 64-75. https://doi.org/10.1196/annals.1392.021

Wohrer, S., Knapp, D. J., Copley, M. R., Benz, C., Kent, D. G., Rowe, K., Babovic, S., Mader, H., Oostendorp, R. A., & Eaves, C. J. (2014). Distinct stromal cell factor combinations can separately control hematopoietic stem cell survival, proliferation, and self-renewal. *Cell Rep*, *7*(6), 1956-1967. https://doi.org/10.1016/j.celrep.2014.05.014

Xavier, C. P., Melikova, M., Chuman, Y., Uren, A., Baljinnyam, B., & Rubin, J. S. (2014). Secreted Frizzled-related protein potentiation versus inhibition of Wnt3a/beta-catenin signaling. *Cell Signal*, *26*(1), 94-101. https://doi.org/10.1016/j.cellsig.2013.09.016

Xie, Y., Yin, T., Wiegraebe, W., He, X. C., Miller, D., Stark, D., Perko, K., Alexander, R., Schwartz, J., Grindley, J. C., Park, J., Haug, J. S., Wunderlich, J. P., Li, H., Zhang, S., Johnson, T., Feldman, R. A., & Li, L. (2009). Detection of functional haematopoietic stem cell niche using real-time imaging. *Nature*, *457*(7225), 97-101. https://doi.org/10.1038/nature07639

Yu, M., Qin, K., Fan, J., Zhao, G., Zhao, P., Zeng, W., Chen, C., Wang, A., Wang, Y., Zhong, J., Zhu, Y., Wagstaff, W., Haydon, R. C., Luu, H. H., Ho, S., Lee, M. J., Strelzow, J., Reid, R. R., & He, T. C. (2024). The evolving roles of Wnt signaling in stem cell proliferation and differentiation, the development of human diseases, and therapeutic opportunities. *Genes Dis*, *11*(3), 101026. https://doi.org/10.1016/j.gendis.2023.04.042

Zhang, Y., Gao, S., Xia, J., & Liu, F. (2018). Hematopoietic Hierarchy - An Updated Roadmap. *Trends Cell Biol*, *28*(12), 976-986. https://doi.org/10.1016/j.tcb.2018.06.001

Zhou, Y., Chen, H., Liu, L., Yu, X., Sukhova, G. K., Yang, M., Kyttaris, V. C., Stillman, I. E., Gelb, B., Libby, P., Tsokos, G. C., & Shi, G. P. (2017). Cathepsin K Deficiency Ameliorates Systemic Lupus Erythematosus-like Manifestations in Fas(lpr) Mice. *J Immunol*, *198*(5), 1846-1854. https://doi.org/10.4049/jimmunol.1501145